Implementation of screened hybrid functionals based on the Yukawa potential within the LAPW basis set

Fabien Tran and Peter Blaha
Institute of Materials Chemistry, Vienna University of Technology, Getreidemarkt 9/165-TC, A-1060 Vienna, Austria

The implementation of screened hybrid functionals into the WIEN2K code, which is based on the LAPW basis set, is reported. The Hartree-Fock exchange energy and potential are screened by means of the Yukawa potential as proposed by Bylander and Kleinman [Phys. Rev. B **41**, 7868 (1990)] for the calculation of the electronic structure of solids with the screened-exchange local density approximation. Details of the formalism, which is based on the method of Massidda, Posternak, and Baldereschi [Phys. Rev. B **48**, 5058 (1993)] for the unscreened Hartree-Fock exchange are given. The results for the transition-energy and structural properties of several test cases are presented. Results of calculations of the Cu electric-field gradient in Cu_2O are also presented, and it is shown that the hybrid functionals are much more accurate than the standard local-density or generalized gradient approximations.

PACS numbers: 71.15.Ap, 71.15.Dx, 71.15.Mb

I. INTRODUCTION

Until now, most Kohn-Sham (KS) density functional theory (DFT)[1,2] calculations on solids have been done using either the local density approximation (LDA) or the generalized gradient approximation (GGA) for the exchange-correlation energy. Calculations were done exclusively with LDA[2] until the early 90s, when the GGA functional PW91[3] was proposed and then implemented in computer codes for solid-state calculations. A few years later, a GGA functional with a simpler analytical form than PW91, namely PBE,[4] but giving nearly identical results has been proposed and is nowadays the standard functional. The successes of the semilocal LDA and GGA approximations rely on the fact that the accuracy is usually good enough to be useful, in particular for the calculation of the geometrical parameters and other quantities like the bulk modulus or the phonon spectrum. (See, e.g., Refs. 5 and 6 for a compilation of lattice constants and bulk moduli calculated with various GGA functionals.) However, it is known that there are classes of systems, e.g., strongly correlated or van der Waals systems, whose properties are not described properly by semilocal functionals already at the qualitative level.

It is also well known that the KS band gap, defined as the conduction band minimum (CBM) minus the valence band maximum (VBM), obtained from a semilocal functional is much smaller than the experimental band gap (defined as the ionization potential I minus the electron affinity A). However, it is important to note that this problem, known as the *band gap problem*, is more general and has its roots in the KS-DFT method itself, and actually the KS band gap calculated with the *exact multiplicative* KS potential would differ from $I - A$ by the derivative discontinuity $\Delta_{\rm xc}$ of the exchange-correlation potential (see Ref. 7 for a review). Since $\Delta_{\rm xc}$ can be of the same order as the KS band gap, the *exact* KS band gap can differ substantially from $I - A$.

There are several methods to obtain orbital energies which lead to values for CBM − VBM comparable to $I - A$. If one wants to stay inside the true KS framework (i.e., KS equations with a multiplicative potential), exact exchange (EXX) calculations (see, e.g., Refs. 8 and 9) or advanced semilocal potentials[10] can do a good job. Alternatively one can use a non-multiplicative potential, which means to use a method which lies outside the KS framework, but belongs to the so-called generalized KS framework.[11] Most of these methods mix the DFT and Hartree-Fock (HF) theories and the best known are the LDA+U,[12] screened-exchange LDA (sX-LDA),[13] and hybrid[14,15] methods. The *GW* method can yield very accurate band structures, in particular if it is applied self-consistently, but it is a very expensive method (see Ref. 16 for a review).

The LDA+U method (see Ref. 17 for a recent review) consists of applying an approximate (but very cheap) form of HF only to the electrons which are not well described by semilocal functionals. Typical examples are the $3d$ or $4f$ electrons in strongly correlated systems (e.g., transition-metal and rare-earth oxides) that are very localized and hence lead to large self-interaction error when a semilocal functional is used (this results in too small band gaps and magnetic moments). In the sX-LDA method, the short-range (SR) part of LDA exchange is replaced by the SR part of HF exchange, where the SR part is defined by replacing the bare Coulomb potential by the screened Yukawa potential[18] into the corresponding expressions for the energy and potential. The sX-LDA method has been implemented within the pseudopotential plane-wave[11,13,19,20] and linearized-augmented plane-wave[21–23] basis sets, and it has been shown that sX-LDA improves substantially over LDA for the band gap of semiconductors and insulators.

Despite the fact that reports about the implementation of the HF method in solid-state codes started to appear already in the 70s (see, e.g., Refs. 24–27), it is only in the early 2000s that the first calculations on solids with

hybrid methods were reported,[28–30] which is much later than for molecules.[14,15] In hybrid methods, a certain percentage (between 10% and 50%) of semilocal exchange is replaced by HF exchange, while the correlation remains purely semilocal. As for molecules, the hybrid functionals have shown to lead to (much) better results than semilocal functionals for various types of materials and properties. In particular, they lead to band structures which are usually in good agreement with experiment as shown for classical semiconductors and insulators (see, e.g., Refs. 28,29,31) and strongly correlated materials (see, e.g., Refs. 28,30–34). The most common hybrid functionals are B3LYP[15,35] and PBE0[36,37] which contain 20% and 25% of HF exchange, respectively. However, for solids the long-range (LR) nature of HF exchange leads to technical difficulties. For calculations done in real space, the results converge very slowly with respect to the number of neighboring unit cells that are taken into account for the calculation of HF exchange, while for calculations done in reciprocal space, the slow convergence is with respect to the number of **k**-points for the integrations in the Brillouin zone.

To reduce this problem of slow convergence, Heyd *et al.* (HSE)[38–40] proposed to consider only the SR part of HF exchange (as done in sX-LDA), and therefore to keep 100% of semilocal LR exchange. This was done by splitting the Coulomb operator into SR and LR components by using the error function.[41,42] Since then, it has been shown that the HSE functional, which is based on PBE0, leads to very good results for semiconductors and insulators[43–47] including strongly correlated systems,[48] and several recent papers reporting the implementation of HSE have appeared.[44,49] We also mention the onsite version of HF exchange proposed by Novák *et al.*,[50] which leads to very cheap calculations, but can be applied only to localized electrons. This method has been used in the context of hybrid calculations.[51,52]

In the present work, we report the implementation of screened hybrid functionals into the WIEN2K code,[53] which is based on the full-potential linearized augmented plane-wave plus local orbitals method (abbreviated as LAPW in the following)[54–57] to solve the KS equations. As done for the sX-LDA functional,[13] the HF exchange is screened by means of the Yukawa potential in order to eliminate the LR HF exchange. The calculation of the screened HF exchange is based on the pseudocharge method[58] as proposed by Massidda *et al.* for the unscreened HF exchange.[27] In the papers of Asahi *et al.*[21,22] it is mentioned that this mehod was used for the implementation of the sX-LDA functional, but only very few details are given. At this point we also mention Refs. 59–62, in which alternative ways of implementing the HF or EXX methods within the LAPW basis set are presented.

The paper is organized as follows: in Sec. II, the details of the formalism of the unscreened and screened HF exchange for the LAPW basis set are given and in Sec. III, the implemented screened hybrid functionals are presented. In Sec. IV, the results for a few test cases and Cu_2O are presented, and in Sec. V the summary of the work is given.

II. SCREENED HARTREE-FOCK EXCHANGE

In this section, the formulas of the screened HF energy for the LAPW basis set are given. The formulas are also valid (and implemented) for the APW plus local orbitals basis set.[56,57] For completeness and to allow comparison, the formulas for the unscreened case are also given. For the Hamiltonian, only the basic formulas are given. The LAPW method will not be described here, but details can be found in Refs. 55–57.

A. Energy

The HF exchange energy per unit cell (of volume Ω) is given by (all following equations are in Hartree atomic units)

$$E_{\rm x}^{\rm HF} = E_{\rm x,vv}^{\rm HF} + E_{\rm x,vc}^{\rm HF} + E_{\rm x,cc}^{\rm HF}, \tag{1}$$

where

$$E_{\rm x,vv}^{\rm HF} = -\frac{1}{2}\sum_{\sigma}\sum_{n,\mathbf{k},n',\mathbf{k}'} w_{n\mathbf{k}}^{\sigma} w_{n'\mathbf{k}'}^{\sigma} \int_{\Omega}\int_{\rm crystal} \psi_{n\mathbf{k}}^{\sigma *}(\mathbf{r})\psi_{n'\mathbf{k}'}^{\sigma}(\mathbf{r}) v\left(|\mathbf{r}-\mathbf{r}'|\right) \psi_{n'\mathbf{k}'}^{\sigma *}(\mathbf{r}')\psi_{n\mathbf{k}}^{\sigma}(\mathbf{r}') d^3r' d^3r, \tag{2}$$

$$E_{\rm x,vc}^{\rm HF} = -\sum_{\sigma}\sum_{\alpha}^{\rm cell}\sum_{n_{\rm c},\ell_{\rm c},m_{\rm c}}\sum_{n,\mathbf{k}} w_{n\mathbf{k}}^{\sigma} \int_{\rm S_\alpha}\int_{\rm S_\alpha} \psi_{n\mathbf{k}}^{\sigma *}(\mathbf{r})\psi_{n_{\rm c}\ell_{\rm c}m_{\rm c}}^{\alpha\sigma}(\mathbf{r}) v\left(|\mathbf{r}-\mathbf{r}'|\right) \psi_{n_{\rm c}\ell_{\rm c}m_{\rm c}}^{\alpha\sigma *}(\mathbf{r}')\psi_{n\mathbf{k}}^{\sigma}(\mathbf{r}') d^3r' d^3r, \tag{3}$$

$$E_{\rm x,cc}^{\rm HF} = -\frac{1}{2}\sum_{\sigma}\sum_{\alpha}^{\rm cell}\sum_{\substack{n_{\rm c},\ell_{\rm c},m_{\rm c}\\ n'_{\rm c},\ell'_{\rm c},m'_{\rm c}}} \int_{\rm S_\alpha}\int_{\rm S_\alpha} \psi_{n'_{\rm c}\ell'_{\rm c}m'_{\rm c}}^{\alpha\sigma *}(\mathbf{r})\psi_{n_{\rm c}\ell_{\rm c}m_{\rm c}}^{\alpha\sigma}(\mathbf{r}) v\left(|\mathbf{r}-\mathbf{r}'|\right) \psi_{n_{\rm c}\ell_{\rm c}m_{\rm c}}^{\alpha\sigma *}(\mathbf{r}')\psi_{n'_{\rm c}\ell'_{\rm c}m'_{\rm c}}^{\alpha\sigma}(\mathbf{r}') d^3r' d^3r, \tag{4}$$

are the valence-valence (vv), valence-core (vc), and core-core (cc) terms, respectively. In Eqs. (2) and (3), $w^{\sigma}_{n\mathbf{k}}$ is the product of the $\mathbf{k}$-point weight and the occupation number and $\psi^{\sigma}_{n\mathbf{k}}$ is a spin-σ valence orbital of band index n and wave vector $\mathbf{k}$, whose LAPW basis set expansion in the interstitial (I) and atomic spheres (S_α) is given by ($\mathbf{r}_\alpha = \mathbf{r} - \tau_\alpha$, where τ_α is the position of nucleus α)

$$\psi^{\sigma}_{n\mathbf{k}}(\mathbf{r}) = \sum_{\mathbf{K}} c^{\sigma}_{n,\mathbf{k}+\mathbf{K}} \phi^{\sigma}_{\mathbf{k}+\mathbf{K}}(\mathbf{r}), \tag{5}$$

$$\phi^{\sigma}_{\mathbf{k}+\mathbf{K}}(\mathbf{r}) = \begin{cases} \frac{1}{\sqrt{\Omega}} e^{\mathrm{i}(\mathbf{k}+\mathbf{K})\cdot\mathbf{r}}, & \mathbf{r} \in \mathrm{I} \\ \sum\limits_{\ell,m} \sum\limits_{f} d^{\alpha\sigma\ell m}_{f,\mathbf{k}+\mathbf{K}} u^{\alpha\sigma}_{f\ell}(r_\alpha) Y_{\ell m}(\hat{\mathbf{r}}_\alpha), & \mathbf{r} \in \mathrm{S}_\alpha \end{cases}, \tag{6}$$

where $c^{\sigma}_{n,\mathbf{k}+\mathbf{K}}$ are the variational coefficients. In the interstitial, the basis functions $\phi^{\sigma}_{\mathbf{k}+\mathbf{K}}$ are represented by plane-waves, while inside the atomic spheres, $\phi^{\sigma}_{\mathbf{k}+\mathbf{K}}$ are linear combinations of products of radial functions $u^{\alpha\sigma}_{f\ell}$ and spherical harmonics $Y_{\ell m}$. The coefficients $d^{\alpha\sigma\ell m}_{f,\mathbf{k}+\mathbf{K}}$ are determined such that the $\phi^{\sigma}_{\mathbf{k}+\mathbf{K}}$'s are continuous across the sphere boundaries. For $f = 1$, 2, and 3, $u^{\alpha\sigma}_{f\ell}$ represents a radial function evaluated at a linearization energy, its energy derivative evaluated at this same energy, and a radial function evaluated at another linearization energy (e.g., semicore states), respectively. In Eqs. (3) and (4), $\psi^{\alpha\sigma}_{n_\mathrm{c},\ell_\mathrm{c},m_\mathrm{c}}$ is a core orbital which is confined inside the atomic sphere S_α and where n_c, ℓ_c, and m_c are the principal, azimuthal, and magnetic quantum numbers, respectively:

$$\psi^{\alpha\sigma}_{n_\mathrm{c}\ell_\mathrm{c}m_\mathrm{c}}(\mathbf{r}) = u^{\alpha\sigma}_{n_\mathrm{c}\ell_\mathrm{c}}(r_\alpha) Y_{\ell_\mathrm{c}m_\mathrm{c}}(\hat{\mathbf{r}}_\alpha). \tag{7}$$

In Eqs. (2)-(4), v is either the unscreened potential

$$\frac{1}{|\mathbf{r}-\mathbf{r}'|} = \sum_{\ell=0}^{\infty} \sum_{m=-\ell}^{\ell} \frac{4\pi}{2\ell+1} \frac{r^{\ell}_{<}}{r^{\ell+1}_{>}} Y^{*}_{\ell m}(\hat{\mathbf{r}}) Y_{\ell m}(\hat{\mathbf{r}}') \tag{8}$$

or the Yukawa screened potential[18]

$$\begin{aligned} \frac{e^{-\lambda|\mathbf{r}-\mathbf{r}'|}}{|\mathbf{r}-\mathbf{r}'|} &= 4\pi\lambda \sum_{\ell=0}^{\infty} \sum_{m=-\ell}^{\ell} i_\ell(\lambda r_<) k_\ell(\lambda r_>) \\ &\quad \times Y^{*}_{\ell m}(\hat{\mathbf{r}}) Y_{\ell m}(\hat{\mathbf{r}}'), \end{aligned} \tag{9}$$

where λ is the screening parameter and i_ℓ and k_ℓ are spherical modified Bessel functions.[63] Note that the spherical harmonics expansion of the screened potential[63] is simpler than in the case of the error function.[64]

1. Valence-valence term

Following the idea of Massidda *et al.*[27] the valence-valence term [Eq. (2)] is cast into the following form

$$\begin{aligned} E^{\mathrm{HF}}_{\mathrm{x,vv}} &= -\frac{1}{2} \sum_{\sigma} \sum_{n,\mathbf{k},n',\mathbf{k}'} w^{\sigma}_{n\mathbf{k}} w^{\sigma}_{n'\mathbf{k}'} \\ &\quad \times \int_{\Omega} \rho^{\sigma}_{n\mathbf{k}n'\mathbf{k}'}(\mathbf{r}) v^{\sigma *}_{n\mathbf{k}n'\mathbf{k}'}(\mathbf{r}) d^3 r, \end{aligned} \tag{10}$$

where

$$\rho^{\sigma}_{n\mathbf{k}n'\mathbf{k}'}(\mathbf{r}) = \psi^{\sigma *}_{n\mathbf{k}}(\mathbf{r}) \psi^{\sigma}_{n'\mathbf{k}'}(\mathbf{r}), \tag{11}$$

and

$$v^{\sigma}_{n\mathbf{k}n'\mathbf{k}'}(\mathbf{r}) = \int_{\text{crystal}} \rho^{\sigma}_{n\mathbf{k}n'\mathbf{k}'}(\mathbf{r}') v(|\mathbf{r}-\mathbf{r}'|)\, d^3 r'. \tag{12}$$

In the interstitial and spheres, $\rho^{\sigma}_{n\mathbf{k}n'\mathbf{k}'}$ and $v^{\sigma}_{n\mathbf{k}n'\mathbf{k}'}$ are expanded in Fourier and spherical harmonics series, respectively (from now on, the index α of the position $\mathbf{r}_\alpha$ from the nucleus α is suppressed and we define $\mathbf{q} = \mathbf{k}' - \mathbf{k} + \mathbf{G}$):

$$\rho^{\sigma}_{n\mathbf{k}n'\mathbf{k}'}(\mathbf{r}) = \begin{cases} \sum\limits_{\mathbf{G}} \rho^{\sigma\mathbf{G}}_{n\mathbf{k}n'\mathbf{k}'} e^{\mathrm{i}\mathbf{q}\cdot\mathbf{r}}, & \mathbf{r} \in \mathrm{I} \\ \sum\limits_{\ell,m} \rho^{\alpha\sigma\ell m}_{n\mathbf{k}n'\mathbf{k}'}(r) Y_{\ell m}(\hat{\mathbf{r}}), & \mathbf{r} \in \mathrm{S}_\alpha \end{cases}, \tag{13}$$

$$v^{\sigma}_{n\mathbf{k}n'\mathbf{k}'}(\mathbf{r}) = \begin{cases} \sum\limits_{\mathbf{G}} v^{\sigma\mathbf{q}}_{n\mathbf{k}n'\mathbf{k}'} e^{\mathrm{i}\mathbf{q}\cdot\mathbf{r}}, & \mathbf{r} \in \mathrm{I} \\ \sum\limits_{\ell,m} v^{\alpha\sigma\ell m}_{n\mathbf{k}n'\mathbf{k}'}(r) Y_{\ell m}(\hat{\mathbf{r}}), & \mathbf{r} \in \mathrm{S}_\alpha \end{cases}. \tag{14}$$

In Eq. (13), $\rho^{\sigma\mathbf{G}}_{n\mathbf{k}n'\mathbf{k}'}$ are the Fourier coefficients of the periodic part of $\rho^{\sigma}_{n\mathbf{k}n'\mathbf{k}'}$ and $\rho^{\alpha\sigma\ell m}_{n\mathbf{k}n'\mathbf{k}'}$ is given by

$$\rho^{\alpha\sigma\ell m}_{n\mathbf{k}n'\mathbf{k}'}(r) = \sum_{\ell_1,\ell_2} \sum_{f_1,f_2} T^{f_1 f_2 \ell_1 \ell_2 \ell m}_{\alpha\sigma n\mathbf{k}n'\mathbf{k}'} u^{\alpha\sigma}_{f_1\ell_1}(r) u^{\alpha\sigma}_{f_2\ell_2}(r), \tag{15}$$

where

$$\begin{aligned} T^{f_1 f_2 \ell_1 \ell_2 \ell m}_{\alpha\sigma n\mathbf{k}n'\mathbf{k}'} &= \sum_{m_1=-\ell_1}^{\ell_1} \sum_{m_2=-\ell_2}^{\ell_2} C^{\ell_2 m_2}_{\ell_1 m_1 \ell m} \\ &\quad \times \left(D^{\alpha\sigma n\mathbf{k} f_1}_{\ell_1 m_1} \right)^{*} D^{\alpha\sigma n'\mathbf{k}' f_2}_{\ell_2 m_2} \end{aligned} \tag{16}$$

with $C^{\ell_2 m_2}_{\ell_1 m_1 \ell m}$ being Gaunt coefficients,

$$C^{\ell_2 m_2}_{\ell_1 m_1 \ell m} = \int_0^{2\pi} \int_0^{\pi} Y^{*}_{\ell_2 m_2}(\hat{\mathbf{r}}) Y_{\ell_1 m_1}(\hat{\mathbf{r}}) Y_{\ell m}(\hat{\mathbf{r}}) \sin\theta d\theta d\phi, \tag{17}$$

and $D^{\alpha\sigma n\mathbf{k} f}_{\ell m} = \sum_{\mathbf{K}} c^{\sigma}_{n,\mathbf{k}+\mathbf{K}} d^{\alpha\sigma\ell m}_{f,\mathbf{k}+\mathbf{K}}$.

$v^{\sigma}_{n\mathbf{k}n'\mathbf{k}'}$ is calculated by using Weinert's method for solving the Poisson equation.[58] (In Appendix A 1, a brief summary of Weinert's method for the unscreened and screened potentials is given.) For the unscreened and screened potentials, the Fourier coefficients $v^{\sigma\mathbf{q}}_{n\mathbf{k}n'\mathbf{k}'}$ are given by

$$v^{\sigma\mathbf{q}}_{n\mathbf{k}n'\mathbf{k}'} = 4\pi \frac{\tilde{\rho}^{\sigma\mathbf{q}}_{n\mathbf{k}n'\mathbf{k}'}}{|\mathbf{q}|^2} \tag{18}$$

and

$$v^{\sigma\mathbf{q}}_{n\mathbf{k}n'\mathbf{k}'} = 4\pi \frac{\tilde{\rho}^{\sigma\mathbf{q}}_{n\mathbf{k}n'\mathbf{k}'}}{|\mathbf{q}|^2 + \lambda^2}, \tag{19}$$

respectively, where $\tilde{\rho}^{\sigma\mathbf{q}}_{n\mathbf{k}n'\mathbf{k}'}$ are the Fourier coefficients of the pseudocharge density [see Eqs. (A9)-(A13) of Appendix A 2]. Note that for the unscreened potential, the term corresponding to $\mathbf{q}=\mathbf{0}$ (i.e., $\mathbf{k}=\mathbf{k}'$ and $\mathbf{G}=\mathbf{0}$) leads to a singularity which has to be considered carefully (details are given at the end of this section).

The radial function $v^{\alpha\sigma\ell m}_{n\mathbf{k}n'\mathbf{k}'}$ is given by [$r_<=\min(r,r')$, $r_>=\max(r,r')$, and R_α is the radius of the atomic sphere]

$$\begin{aligned} v^{\alpha\sigma\ell m}_{n\mathbf{k}n'\mathbf{k}'}(r) &= \int_0^{R_\alpha} \rho^{\alpha\sigma\ell m}_{n\mathbf{k}n'\mathbf{k}'}(r') G^\alpha_\ell(r,r')\, r'^2 dr' \\ &\quad + v^{\alpha\sigma\ell m}_{n\mathbf{k}n'\mathbf{k}'}(R_\alpha) P_\ell(r), \end{aligned} \tag{20}$$

where G^α_ℓ is Eq. (A7) and $P_\ell = r^\ell/R^\ell_\alpha$ for the unscreened potential or G^α_ℓ is Eq. (A8) and $P_\ell = i_\ell(\lambda r)/i_\ell(\lambda R_\alpha)$ for the screened potential. In Eq. (20),

$$v^{\alpha\sigma\ell m}_{n\mathbf{k}n'\mathbf{k}'}(R_\alpha) = 4\pi \mathrm{i}^\ell \sum_{\mathbf{G}} v^{\sigma\mathbf{q}}_{n\mathbf{k}n'\mathbf{k}'} e^{\mathrm{i}\mathbf{q}\cdot\tau_\alpha} Y^*_{\ell m}(\hat{\mathbf{q}})\, j_\ell(|\mathbf{q}| R_\alpha), \tag{21}$$

which is obtained by using the Rayleigh formula[63]

$$e^{\mathrm{i}\mathbf{q}\cdot\mathbf{r}} = 4\pi \sum_{\ell=0}^{\infty} \sum_{m=-\ell}^{\ell} \mathrm{i}^\ell j_\ell(|\mathbf{q}| r)\, Y^*_{\ell m}(\hat{\mathbf{q}})\, Y_{\ell m}(\hat{\mathbf{r}}) \tag{22}$$

in the Fourier expansion of $v^\sigma_{n\mathbf{k}n'\mathbf{k}'}$ [Eq. (14)], where j_ℓ is a spherical Bessel function.[63]

$E^{\mathrm{HF}}_{\mathrm{x,vv}}$ is decomposed into its interstitial and atomic sphere parts:

$$E^{\mathrm{HF}}_{\mathrm{x,vv}} = E^{\mathrm{HF,I}}_{\mathrm{x,vv}} + \sum_\alpha^{\mathrm{cell}} E^{\mathrm{HF,S}_\alpha}_{\mathrm{x,vv}}, \tag{23}$$

where

$$\begin{aligned} E^{\mathrm{HF,I}}_{\mathrm{x,vv}} &= -\frac{1}{2}\sum_\sigma \sum_{n,\mathbf{k},n',\mathbf{k}'} w^\sigma_{n\mathbf{k}} w^\sigma_{n'\mathbf{k}'} \\ &\quad \times \int_\Omega \rho^\sigma_{n\mathbf{k}n'\mathbf{k}'}(\mathbf{r}) v^{\sigma *}_{n\mathbf{k}n'\mathbf{k}'}(\mathbf{r}) \Theta(\mathbf{r}) d^3r \\ &= -\frac{\Omega}{2}\sum_\sigma \sum_{n,\mathbf{k},n',\mathbf{k}'} w^\sigma_{n\mathbf{k}} w^\sigma_{n'\mathbf{k}'} \\ &\quad \times \sum_{\mathbf{G}} (\rho^\sigma_{n\mathbf{k}n'\mathbf{k}'} v^{\sigma *}_{n\mathbf{k}n'\mathbf{k}'})_{\mathbf{G}}\, \Theta_{-\mathbf{G}}, \end{aligned} \tag{24}$$

with $\Theta(\mathbf{r})=1$ if $\mathbf{r}\in \mathrm{I}$ and 0 if $\mathbf{r}\in \mathrm{S}_\alpha$, whose Fourier transform $\Theta_{\mathbf{G}}$ is given by

$$\Theta_{\mathbf{G}} = \begin{cases} -\frac{4\pi}{\Omega}\sum_\alpha^{\mathrm{cell}} e^{-\mathrm{i}\mathbf{G}\cdot\tau_\alpha} R^3_\alpha \frac{j_1(|\mathbf{G}|R_\alpha)}{|\mathbf{G}|R_\alpha}, & \mathbf{G}\neq\mathbf{0} \\ 1-\frac{4\pi}{3\Omega}\sum_\alpha^{\mathrm{cell}} R^3_\alpha, & \mathbf{G}=\mathbf{0} \end{cases}, \tag{25}$$

and

$$\begin{aligned} E^{\mathrm{HF,S}_\alpha}_{\mathrm{x,vv}} &= -\frac{1}{2}\sum_\sigma \sum_{n,\mathbf{k},n',\mathbf{k}'} w^\sigma_{n\mathbf{k}} w^\sigma_{n'\mathbf{k}'} \int_{\mathrm{S}_\alpha} \rho^\sigma_{n\mathbf{k}n'\mathbf{k}'}(\mathbf{r}) v^{\sigma *}_{n\mathbf{k}n'\mathbf{k}'}(\mathbf{r}) d^3r \\ &= -\frac{1}{2}\sum_\sigma \sum_{n,\mathbf{k},n',\mathbf{k}'} w^\sigma_{n\mathbf{k}} w^\sigma_{n'\mathbf{k}'} \sum_{\ell,m} \Bigg[\sum_{\substack{\ell_1,\ell_2\\ \ell_3,\ell_4}} \sum_{\substack{f_1,f_2\\ f_3,f_4}} T^{f_1 f_2 \ell_1 \ell_2 \ell m}_{\alpha\sigma n\mathbf{k}n'\mathbf{k}'} \left(T^{f_3 f_4 \ell_3 \ell_4 \ell m}_{\alpha\sigma n\mathbf{k}n'\mathbf{k}'}\right)^* \\ &\quad \times \int_0^{R_\alpha}\int_0^{R_\alpha} u^{\alpha\sigma}_{f_1\ell_1}(r) u^{\alpha\sigma}_{f_2\ell_2}(r) G^\alpha_\ell(r,r') u^{\alpha\sigma}_{f_3\ell_3}(r') u^{\alpha\sigma}_{f_4\ell_4}(r') r^2 r'^2 dr' dr + Q_\ell q^{\alpha\sigma n\mathbf{k}n'\mathbf{k}'}_{\ell m} v^{\alpha\sigma\ell m *}_{n\mathbf{k}n'\mathbf{k}'}(R_\alpha) \Bigg], \end{aligned} \tag{26}$$

where $Q_\ell = 1/R^\ell_\alpha$ and $q^{\alpha\sigma n\mathbf{k}n'\mathbf{k}'}_{\ell m}$ is Eq. (A15) for the unscreened potential or $Q_\ell = (1/i_\ell(\lambda R_\alpha))\,\lambda^\ell/(2\ell+1)!!$ and $q^{\alpha\sigma n\mathbf{k}n'\mathbf{k}'}_{\ell m}$ is Eq. (A17) for the screened potential.

As already mentioned above, the singularity which arises when $\mathbf{q}=\mathbf{0}$ [see Eq. (18)] needs to be considered properly. Several methods to deal with this integrable singularity when integrating into the Brillouin zone are available in the literature[27,60,65–69] and have been used in very recent studies.[61,70–75] We adopted the simple scheme proposed by Spencer and Alavi[69] which consists of multiplying Eq. (18) by $1-\cos(|\mathbf{q}| R_\mathrm{c})$, where $R_\mathrm{c} = (3/(4\pi) N_{\mathbf{k}}\Omega)^{1/3}$ with $N_{\mathbf{k}}$ being the number of $\mathbf{k}$-points in the full Brillouin zone. In the real space this corresponds to multiplying Eq. (8) by the step function $\theta(R_\mathrm{c}-|\mathbf{r}-\mathbf{r}'|)$.[69] By doing this, the term $\mathbf{q}=\mathbf{0}$ tends to a finite value:

$$\lim_{|\mathbf{q}|\to 0} \frac{4\pi}{|\mathbf{q}|^2}(1-\cos(|\mathbf{q}| R_\mathrm{c})) = 2\pi R^2_\mathrm{c}, \tag{27}$$

which leads to a much more faster convergence (with respect to $N_{\mathbf{k}}$) of the integrations into the Brillouin zone.

The screened potential has no singularity at $\mathbf{q}=\mathbf{0}$ [see Eq. (19)], nevertheless it is still useful to apply the same technique in order to accelerate further the convergence

of the integrations into the Brillouin zone. Multiplying Eq. (9) by the step function $\theta(R_\mathrm{c} - |\mathbf{r} - \mathbf{r}'|)$ means that in the reciprocal space Eq. (19) should be multiplied by

$$1 - e^{-\lambda R_\mathrm{c}} \left(\frac{\lambda}{|\mathbf{q}|} \sin\left(|\mathbf{q}|\, R_\mathrm{c}\right) + \cos\left(|\mathbf{q}|\, R_\mathrm{c}\right) \right), \tag{28}$$

which becomes $1 - e^{-\lambda R_\mathrm{c}} \left(\lambda R_\mathrm{c} + 1\right)$ at $\mathbf{q} = \mathbf{0}$.

2. *Valence-core and core-core terms*

By supposing that the core shells are closed (see Refs. 24 and 27), the Legendre polynomial addition theorem[63] can be used to simplify the calculation of the valence-core and core-core terms of the HF exchange energy [Eqs. (3) and (4)]. The final expressions are given by

$$\begin{aligned} E^\mathrm{HF}_\mathrm{x,vc} \;=\; & -\sum_\sigma \sum_\alpha^\mathrm{cell} \sum_{n_\mathrm{c},\ell_\mathrm{c}} \sum_{n,\mathbf{k}} \sum_{\ell,\ell',m'} \sum_{f_1,f_2} w^\sigma_{n\mathbf{k}} \left(D^{\alpha\sigma n\mathbf{k}f_1}_{\ell' m'} \right)^* D^{\alpha\sigma n\mathbf{k}f_2}_{\ell' m'} C^{\ell' 0}_{\ell 0 \ell_\mathrm{c} 0} \sqrt{\frac{(2\ell_\mathrm{c}+1)\,(2\ell+1)}{4\pi\,(2\ell'+1)}} \\ & \times \int_0^{R_\alpha} \int_0^{R_\alpha} u^{\alpha\sigma}_{f_1\ell'}(r) u^{\alpha\sigma}_{n_\mathrm{c}\ell_\mathrm{c}}(r) H_\ell(r,r') u^{\alpha\sigma}_{n_\mathrm{c}\ell_\mathrm{c}}(r') u^{\alpha\sigma}_{f_2\ell'}(r') r^2 r'^2 dr' dr, \end{aligned} \tag{29}$$

$$\begin{aligned} E^\mathrm{HF}_\mathrm{x,cc} \;=\; & -\frac{1}{2} \sum_\sigma \sum_\alpha^\mathrm{cell} \sum_{\substack{n_\mathrm{c},\ell_\mathrm{c} \\ n'_\mathrm{c},\ell'_\mathrm{c}}} \sum_\ell C^{\ell 0}_{\ell_\mathrm{c} 0 \ell'_\mathrm{c} 0} \sqrt{\frac{(2\ell_\mathrm{c}+1)\,(2\ell'_\mathrm{c}+1)\,(2\ell+1)}{4\pi}} \\ & \times \int_0^{R_\alpha} \int_0^{R_\alpha} u^{\alpha\sigma}_{n'_\mathrm{c}\ell'_\mathrm{c}}(r) u^{\alpha\sigma}_{n_\mathrm{c}\ell_\mathrm{c}}(r) H_\ell(r,r') u^{\alpha\sigma}_{n_\mathrm{c}\ell_\mathrm{c}}(r') u^{\alpha\sigma}_{n'_\mathrm{c}\ell'_\mathrm{c}}(r') r^2 r'^2 dr' dr, \end{aligned} \tag{30}$$

where $H_\ell(r,r') = \left(4\pi/\left(2\ell+1\right)\right) r_<^\ell / r_>^{\ell+1}$ for the unscreened potential or $H_\ell(r,r') = 4\pi\lambda i_\ell\left(\lambda r_<\right) k_\ell\left(\lambda r_>\right)$ for the screened potential. $C^{\ell_3 m_3}_{\ell_1 m_1 \ell_2 m_2}$ are Gaunt coefficients [Eq. (17)] and $D^{\alpha\sigma n\mathbf{k}f}_{\ell m}$ were defined in Sec. II A. Note that in Eqs. (29) and (30), all integrations are inside the atomic spheres only, thus the cost for the calculation of these two terms is negligible compared to the valence-valence term.

B. Hamiltonian

The HF exchange operator for the valence orbitals is the sum of the valence-valence and valence-core terms: $\hat{v}^\mathrm{HF}_{\mathrm{x}\sigma} = \hat{v}^\mathrm{HF}_{\mathrm{x}\sigma,\mathrm{vv}} + \hat{v}^\mathrm{HF}_{\mathrm{x}\sigma,\mathrm{vc}}$. For the present work we chose to implement the HF (and hybrid, see Sec. III) operator using a second variational procedure, which consists of using the semilocal (SL), LDA or GGA, orbitals as basis functions for the calculation of the matrix elements of the perturbation operator $\langle \psi^{\sigma\mathrm{SL}}_{n\mathbf{k}} | \hat{v}^\mathrm{HF}_{\mathrm{x}\sigma} - v^\mathrm{SL}_{\mathrm{x}\sigma} | \psi^{\sigma\mathrm{SL}}_{n'\mathbf{k}} \rangle$. The HF part is given by

$$\langle \psi^{\sigma\mathrm{SL}}_{n\mathbf{k}} | \hat{v}^\mathrm{HF}_{\mathrm{x}\sigma,\mathrm{vv}} | \psi^{\sigma\mathrm{SL}}_{n'\mathbf{k}} \rangle = -\sum_{n'',\mathbf{k}''} w^\sigma_{n''\mathbf{k}''} \int_\Omega \int_\mathrm{crystal} \psi^{\sigma\mathrm{SL}*}_{n\mathbf{k}}(\mathbf{r}) \psi^\sigma_{n''\mathbf{k}''}(\mathbf{r}) v\left(|\mathbf{r}-\mathbf{r}'|\right) \psi^{\sigma *}_{n''\mathbf{k}''}(\mathbf{r}') \psi^{\sigma\mathrm{SL}}_{n'\mathbf{k}}(\mathbf{r}') d^3r' d^3r, \tag{31}$$

$$\langle \psi^{\sigma\mathrm{SL}}_{n\mathbf{k}} | \hat{v}^\mathrm{HF}_{\mathrm{x}\sigma,\mathrm{vc}} | \psi^{\sigma\mathrm{SL}}_{n'\mathbf{k}} \rangle = -\sum_\alpha^\mathrm{cell} \sum_{n_\mathrm{c},\ell_\mathrm{c},m_\mathrm{c}} \int_{\mathrm{S}_\alpha} \int_{\mathrm{S}_\alpha} \psi^{\sigma\mathrm{SL}*}_{n\mathbf{k}}(\mathbf{r}) \psi^{\alpha\sigma}_{n_\mathrm{c}\ell_\mathrm{c}m_\mathrm{c}}(\mathbf{r}) v\left(|\mathbf{r}-\mathbf{r}'|\right) \psi^{\alpha\sigma *}_{n_\mathrm{c}\ell_\mathrm{c}m_\mathrm{c}}(\mathbf{r}') \psi^{\sigma\mathrm{SL}}_{n'\mathbf{k}}(\mathbf{r}') d^3r' d^3r, \tag{32}$$

which are calculated using the same procedure as for the HF exchange energy, but with $\rho^\sigma_{n\mathbf{k}n''\mathbf{k}''} = \psi^{\sigma\mathrm{SL}*}_{n\mathbf{k}} \psi^\sigma_{n''\mathbf{k}''}$ for Eq. (31). The second variational procedure, which was

also adopted for the HF implementations in other LAPW codes[21,22,27,61] leads to cheaper calculations, since in practice the number of orbitals $\psi_{n\mathbf{k}}^{\sigma\mathrm{SL}}$ which are used for the construction of the HF Hamiltonian matrix is much smaller than the number of LAPW basis functions. In the present implementation, the core electrons experience the semilocal potential, similarly as what is done in the FLEUR code, where the core electrons are taken from a previous semilocal calculation and kept frozen during the calculation with the hybrid functional.[61]

III. SCREENED HYBRID FUNCTIONALS

In screened hybrid functionals, the SR part of a fraction α_x of semilocal exchange is replaced by SR HF exchange:[38]

$$E_\mathrm{xc} = E_\mathrm{xc}^\mathrm{SL} + \alpha_\mathrm{x}\left(E_\mathrm{x}^\mathrm{SR\text{-}HF} - E_\mathrm{x}^\mathrm{SR\text{-}SL}\right), \qquad (33)$$

where $E_\mathrm{x}^\mathrm{SR\text{-}HF}$ and $E_\mathrm{x}^\mathrm{SR\text{-}SL}$ are obtained by replacing the full (i.e., unscreened) Coulomb operator by the screened (i.e., SR) operator into the corresponding expressions. For the HSE functional,[38] the Coulomb operator was split into SR and LR components by using the error function, however, for the present work we chose to split the Coulomb operator by using the exponential function:

$$\frac{1}{|\mathbf{r}-\mathbf{r}'|} = \underbrace{\frac{e^{-\lambda|\mathbf{r}-\mathbf{r}'|}}{|\mathbf{r}-\mathbf{r}'|}}_{\mathrm{SR}} + \underbrace{\frac{1-e^{-\lambda|\mathbf{r}-\mathbf{r}'|}}{|\mathbf{r}-\mathbf{r}'|}}_{\mathrm{LR}}. \qquad (34)$$

Figure 1 shows the SR and LR parts [Eq. (34)] of the Coulomb potential $1/x = 1/|\mathbf{r}-\mathbf{r}'|$, and for comparison, the same is shown when the error function is used to split $1/x$ [$\mathrm{erfc}(\mu x) = 1-\mathrm{erf}(\mu x)$ is the complementary error function]. In both cases, the screening parameter is set to $\lambda = \mu = 1$. At $x = 0$, the values of the LR parts $\left(1-e^{-\lambda x}\right)/x$ and $\left(1-\mathrm{erfc}(\mu x)\right)/x$ are λ and $2\mu/\sqrt{\pi}$, respectively, thus these two ways of splitting the Coulomb operator lead to LR components which are not zero at $x = 0$. Sharper splitting schemes which lead to a LR component which is zero at $x = 0$ consist of using, e.g., the erfgau function[76] or simply the step function.[69] We mention that for technical convenience, Shimazaki and Asai replaced $e^{-\lambda x}$ by $\mathrm{erfc}((2/3)\lambda x)$ in their proposed screened HF potential.[77–79] Indeed, from Fig. 2 we can see that if $\lambda = (3/2)\,\mu$, the two splitting procedures lead to very similar SR and LR parts. In this example, $\mu = 0.11$ bohr^{-1}, which is the value used for the HSE06 functional.[45]

In Eq. (33), $E_\mathrm{x}^\mathrm{SR\text{-}HF}$ is given by Eqs. (1)-(4) with the Yukawa potential [Eq. (9)] for v and $E_\mathrm{x}^\mathrm{SR\text{-}SL}$ is given by

$$E_\mathrm{x}^\mathrm{SR\text{-}SL} = -\frac{3}{4}\left(\frac{6}{\pi}\right)^{1/3}\sum_\sigma \int_\Omega \rho_\sigma^{4/3}(\mathbf{r}) \times F_\mathrm{x}(s_\sigma(\mathbf{r}))J(a_\sigma(\mathbf{r}))d^3r, \qquad (35)$$

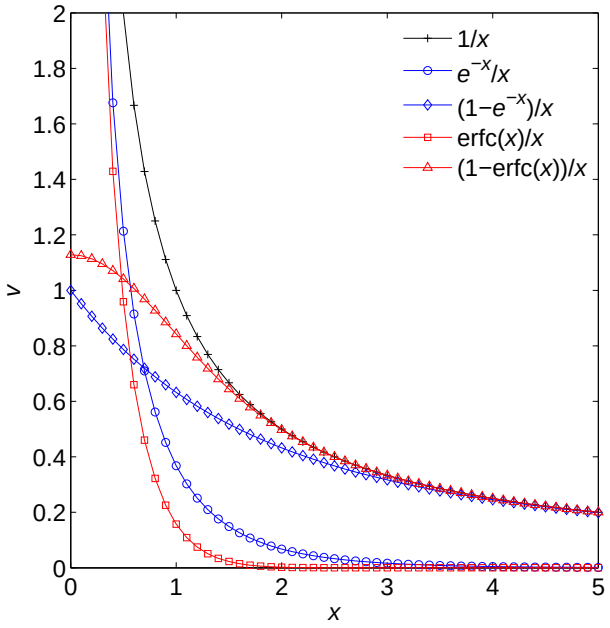

FIG. 1: (Color online) Plots of the SR and LR parts of the Coulomb operator $1/x$, when split using the exponential (in blue) or error (in red) functions.

where $F_\mathrm{x}(s_\sigma)$ [where $s_\sigma = |\nabla\rho_\sigma|/(2\rho_\sigma k_\mathrm{F}^\sigma)$ with $k_\mathrm{F}^\sigma = \left(6\pi^2\rho_\sigma\right)^{1/3}$] is the enhancement factor of the semilocal exchange functional and $J(a_\sigma)$ [where $a_\sigma = \lambda\sqrt{F_\mathrm{x}(s_\sigma)}/(2k_\mathrm{F}^\sigma)$] is a function, whose analytical form depends on the way the Coulomb operator is screened [$J(a_\sigma) = 1$ for the unscreened operator]. In our case [SR part of Eq. (34)], $J(a_\sigma)$ is given by[80]

$$J(a_\sigma) = 1 - \frac{2}{3}a_\sigma^2 - \frac{8}{3}a_\sigma \arctan\frac{1}{a_\sigma} + \frac{2}{3}a_\sigma^2\left(a_\sigma^2+3\right)\ln\left(1+\frac{1}{a_\sigma^2}\right). \qquad (36)$$

Equation (35) is an approximation which was originally proposed by Iikura *et al.*,[81] but with the function $J(a_\sigma)$ for the error function. Recently, Akinaga and Ten-no[82] used Eq. (35) in conjunction with the Yukawa potential as in the present work. (However, we note that in Refs. 81 and 82, this is the LR part of the semilocal exchange which was replaced by LR HF.) A more elegent way of calculating $E_\mathrm{x}^\mathrm{SR\text{-}SL}$ would be to use its expression in terms of the exchange hole (as done for HSE[39,83]), and, for practical convenience, to find a mathematical form for the exchange hole such that an analytical integration with the Yukawa potential is possible, as done in Ref. 84 for the error function. This method has been used in Ref. 85 for the HSEsol functional, which is based on the PBEsol GGA functional.[86] We did not consider this possibility for the present work.

For the semilocal terms in Eq. (33) we have chosen PBE,[4] which is of the GGA form. In the following, this functional will be called YS-PBE0 (where YS stands for

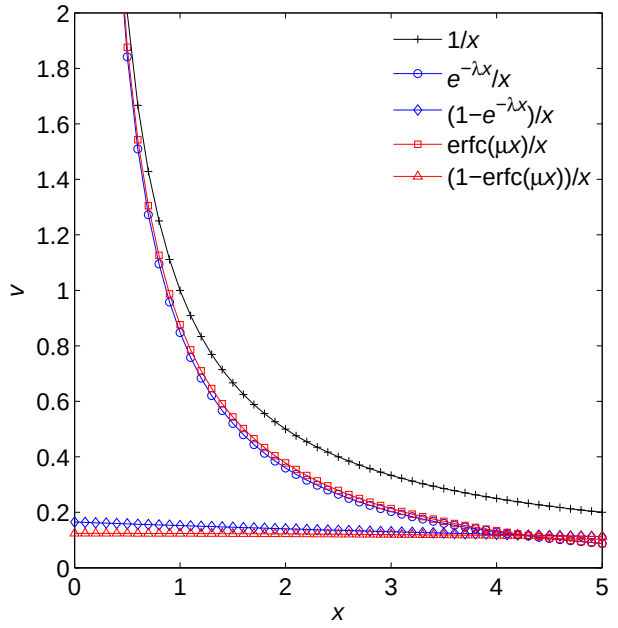

FIG. 2: (Color online) Plots of the SR and LR parts of the Coulomb operator $1/x$, when split using the error (with $\mu = 0.11$ bohr^{-1}) or the exponential [with $\lambda = (3/2)\,\mu = 0.165$ bohr^{-1}] functions.

Yukawa screened). In the literature, the unscreened version of this hybrid functional (recovered when $\lambda \to 0$) is called PBE0,[36,37] for which the fraction of HF exchange is $\alpha_{\rm x} = 0.25$ (see Ref. 87). For $\lambda \to \infty$, YS-PBE0 reduces to PBE. The calculation of the total energy for hybrid functionals is given in Appendix B. As already mentioned in Sec. II B, the second variational procedure has been implemented, and the matrix elements of the perturbation operator corresponding to Eq. (33) are given by

$$\langle \psi^{\sigma\rm SL}_{n\mathbf{k}} | \alpha_{\rm x} \left(\hat{v}^{\rm SR\text{-}HF}_{{\rm x}\sigma} - v^{\rm SR\text{-}SL}_{{\rm x}\sigma} \right) | \psi^{\sigma\rm SL}_{n'\mathbf{k}} \rangle, \qquad (37)$$

where the expression for $v^{\rm SR\text{-}SL}_{{\rm x}\sigma} = \delta E^{\rm SR\text{-}SL}_{\rm x} / \delta \rho_\sigma$ is given in Appendix C.

IV. NUMERICAL RESULTS

The calculations presented in this section were done with values for the parameters such that the results are well converged. The most important parameters are the number of $\mathbf{k}$ points for the integrations into the Brillouin zone, the size of the basis sets (first and second variational procedures), $G_{\rm max}$ and $\ell_{\rm max}$ in Eqs. (13) and (14), and $\ell_{\rm max}$ in Eq. (15). We will not discuss in detail the convergence of the results with respect to these parameters, but just mention the following: for the transition energies and lattice constants, the number of orbitals used as basis functions for the second variational procedure is between two and six times larger than the number of valence bands in the system. The values of $G_{\rm max}$ lie in the range 4−10 bohr^{-1} and for most calculations the value $\ell_{\rm max} = 4$ was used, which is more than enough most of the time. The size of the $\mathbf{k}$-meshes will be mentioned below.

We mention again that the computation of the HF Hamiltonian is very expensive, and for the systems we have considered this leads to computational times which are by one or two orders of magnitude larger than for semilocal functionals. Actually, the values of all parameters mentioned above have a large impact on the computational time.

TABLE I: Total and exchange energies (in Ha) of He atom.

	WIEN2K		Reference	
Functional	$-E_{\rm tot}$	$-E_{\rm x}$	$-E_{\rm tot}$	$-E_{\rm x}$
LDAx[a]	2.724	0.853	2.724	0.853
B88[a]	2.863	1.016	2.863	1.016
PW91x[a]	2.855	1.005	2.855	1.005
HF[a]	2.862	1.024	2.862	1.026
HF[b]		0.998		0.998
HF[c]		1.017		

[a] Obtained from exchange-only self-consistent calculations. The reference results are from Refs. 89 and 91.
[b] Evaluated with LDA (exchange and correlation) orbitals. The reference result is from Ref. 90.
[c] Evaluated with B88PW91 orbitals.

A. Comparison with other codes

1. HF energy

As a first test of the correctness and accuracy of the implementation, we considered systems which do not contain core electrons, such that all electrons are treated self-consistently with the HF method. The He atom and solid LiH are two such systems for which highly accurate HF results are available in the literature. The LDAx (exchange-only LDA) orbitals were used as basis functions for the Hamiltonian of the second variational procedure.

The results for the He atom are shown in Table I. The calculations were done in a fcc cell with a lattice constant of 9.5 Å which is large enough to make the interactions between the He atoms negligible. First, in order to have an idea of the accuracy that can be expected with WIEN2K, we did calculations with semilocal functionals (exchange only: LDAx, B88,[88] and PW91x[3]) and compared them to accurate atomic results.[89,90] From the results we can see that an agreement at the mHa level can be reached, which is the target for the HF calculations. The self-consistent HF results shown in Table I were obtained using 410 bands for the second variational procedure, which was enough to reach convergence and thus agreement with accurate atomic results.[91] However,

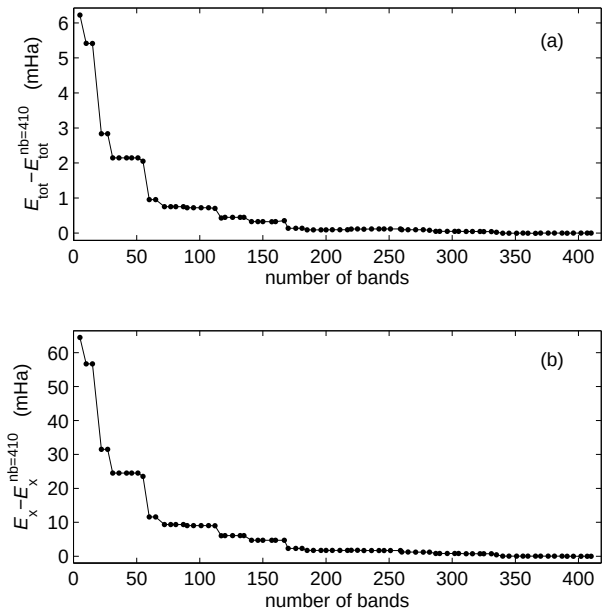

FIG. 3: (a) Total and (b) exchange energy of the He atom with respect to the values calculated with 410 bands.

for the exchange energy $E_{\rm x}$, the agreement with the reference result is not perfect. Actually, we can see in Fig. 3 that for a given number of bands, the error with respect to the (approximately) converged value is ten times larger for the exchange energy than for the total energy. For $E_{\rm tot}$, about 120 bands are necessary to reach convergence at the mHa level, while 410 bands are still not enough for $E_{\rm x}$ (about 3000 LAPW basis functions are used for the first variational procedure). It is known that the total energy converges faster than its components. In order to evaluate the effects due to self-consistency, the HF exchange energy was also evaluated using the LDA (with PW92 for correlation[92]) and B88PW91 (B88[88] for exchange and PW91[3] for correlation) orbitals. From Table I, we can see that using LDA orbitals leads to an HF exchange energy whose magnitude is 26 mHa smaller, while using B88PW91 orbitals leads to a value which is much closer to the self-consistent one, which is maybe not surprising since the empirical parameter in B88 was determined by a fit to HF exchange energy of rare-gas atoms.[88] This indicates that using the B88PW91 orbitals as basis functions for the second-variational Hamiltonian would be more efficient.

In Ref. 74 (as well as in the Comment), well converged calculations on solid LiH (rocksalt structure) using Gaussian basis sets yield a value of $E_{\rm tot} = -8.0645$ Ha at the experimental geometry (4.084 Å). Using a $6 \times 6 \times 6$ **k**-mesh and 65 bands for the second variational procedure we obtained $E_{\rm tot} = -8.0642$ Ha. Increasing further the number of bands would lower the total energy and reduce the difference between the Gaussian and LAPW results. Therefore, as for the He atom, the HF energy calculated with the LAPW code agrees very well with the literature results.

2. PBE0 calculations

In Refs. 44 and 61, calculations with the unscreened hybrid functional PBE0 were done within the projector augmented-wave (VASP code) and LAPW (FLEUR code) methods, respectively. The implementation of the HF equations within the LAPW basis set as reported in Ref. 61 was done using another technique (mixed product basis) as the one used in the present work (pseudocharge method). The integrations into the Brillouin zone were done with a $7 \times 7 \times 7$ **k**-mesh for the semiconductors and insulators, while for the metals Li, Cu, and Rh a $12 \times 12 \times 12$ **k**-mesh was used. The results from Refs. 44 and 61 were done with a $12 \times 12 \times 12$ **k**-mesh, however test calculations indicate that our results are converged within ~ 0.02 eV for the transition energies and ~ 0.002 Å for the lattice constants.

Transition energies were calculated for six solids at the experimental lattice constant: Ar (fcc, 5.260 Å), C (diamond, 3.567 Å), Si (diamond, 5.430 Å), GaAs (zinc blende, 5.648 Å), MgO (rocksalt, 4.207 Å), and NaCl (rocksalt, 5.595 Å). The PBE0 results, as well as the PBE and experimental results, are given in Table II, where we can see that the WIEN2K results agree very well with the FLEUR and VASP results. There are a few cases where the discrepancy is larger than 0.1 eV. For the $\Gamma \rightarrow L$ transition in C, there is a difference of 0.12 eV between the WIEN2K and FLEUR values and in the case of NaCl, a disagreement of 0.15−0.2 eV with FLEUR is found for the $\Gamma \rightarrow \Gamma$ and $\Gamma \rightarrow X$ transitions. Nevertheless, overall the agreement with the FLEUR and VASP codes for the PBE0 hybrid functional is clearly satisfactory, in particular with VASP. Compared to the experimental values, the PBE0 functional clearly improves upon PBE, however, some sizeable disagreements with experiment are still present, as for example for Ar and NaCl for which PBE0 underestimates the $\Gamma \rightarrow \Gamma$ transition by about 3 and 1.2 eV, respectively. In general, the tendency of the PBE0 functional is to overestimate small band gaps (e.g., GaAs) and to underestimate large band gaps (e.g., rare-gas solids).[47]

The lattice constant and bulk modulus of a few selected compounds, namely, Li (bcc), C (diamond), Si (diamond), Cu (fcc), Rh (fcc), LiF (rocksalt), BN (zinc blende), and SiC (zinc blende) were calculated using the PBE and PBE0 functionals. The results are shown in Table III together with the values obtained with the VASP code[44] and the experimental data, which were corrected for the zero-point anharmonic expansion.[85] By comparing the WIEN2K and VASP results, we can see that excellent agreement between the two codes are obtained both for the PBE and PBE0 functionals. The largest discrepancy in the lattice constant is found for Si, where a difference of 0.007−0.01 Å is found for PBE and PBE0. From Table III we can see that there is also a good agree-

TABLE II: Transition energies (in eV) obtained with the PBE, PBE0, and YS-PBE0 ($\lambda = 0.165$ bohr^{-1}) functionals.

		WIEN2K			VASP[a]			FLEUR[b]		
Solid	Transition	PBE	PBE0	YS-PBE0	PBE	PBE0	HSE06	PBE	PBE0	Expt.[c]
Ar	$\Gamma \to \Gamma$	8.69	11.09	10.36	8.68	11.09	10.34	8.71	11.15	14.2
C	$\Gamma \to \Gamma$	5.59	7.69	6.94	5.59	7.69	6.97	5.64	7.74	7.3
	$\Gamma \to X$	4.76	6.64	5.91	4.76	6.66	5.91	4.79	6.69	
	$\Gamma \to L$	8.46	10.76	9.97	8.46	10.77	10.02	8.58	10.88	
Si	$\Gamma \to \Gamma$	2.56	3.95	3.30	2.57	3.97	3.32	2.56	3.96	3.4
	$\Gamma \to X$	0.71	1.91	1.31	0.71	1.93	1.29	0.71	1.93	
	$\Gamma \to L$	1.53	2.86	2.23	1.54	2.88	2.24	1.54	2.87	2.4
GaAs	$\Gamma \to \Gamma$	0.53	1.99	1.39	0.56	2.01	1.45	0.55	2.02	1.63
	$\Gamma \to X$	1.46	2.66	2.08	1.46	2.67	2.02	1.47	2.69	2.18, 2.01
	$\Gamma \to L$	1.01	2.35	1.74	1.02	2.37	1.76	1.02	2.38	1.84, 1.85
MgO	$\Gamma \to \Gamma$	4.79	7.23	6.49	4.75	7.24	6.50	4.84	7.31	7.7
	$\Gamma \to X$	9.16	11.58	10.83	9.15	11.67	10.92	9.15	11.63	
	$\Gamma \to L$	7.95	10.43	9.68	7.91	10.38	9.64	8.01	10.51	
NaCl	$\Gamma \to \Gamma$	5.22	7.29	6.61	5.20	7.26	6.55	5.08	7.13	8.5
	$\Gamma \to X$	7.59	9.80	9.06	7.60	9.66	8.95	7.39	9.59	
	$\Gamma \to L$	7.33	9.40	8.70	7.32	9.41	8.67	7.29	9.33	

[a]Reference 44 (see Erratum for HSE06 results).
[b]Reference 61.
[c]The references for the experimental values are given in Table I of Ref. 61.

TABLE III: Equilibrium lattice constants a_0 (in Å) and bulk moduli B_0 (in GPa) obtained with the PBE, PBE0, and YS-PBE0 ($\lambda = 0.165$ bohr^{-1}) functionals. The experimental values, which are corrected for the zero-point anharmonic expansion, are from Ref. 85.

	WIEN2K						VASP[a]							
	PBE		PBE0		YS-PBE0		PBE		PBE0		HSE06		Expt.	
Solid	a_0	B_0	a_0	B_0	a_0	B_0	a_0	B_0	a_0	B_0	a_0	B_0	a_0	B_0
Li	3.434	13.9	3.464	13.1	3.467	12.6	3.438	13.7	3.463	13.7	3.460	13.6	3.453	13.9
C	3.575	435	3.549	475	3.554	467	3.574	431	3.549	467	3.549	467	3.553	455
Si	5.476	89.0	5.443	99.4	5.459	96.5	5.469	87.8	5.433	99.0	5.435	97.7	5.421	101
Cu	3.631	141	3.630	131	3.654	119	3.635	136	3.636	130	3.638	126	3.595	145
Rh	3.830	256	3.787	292	3.799	280	3.830	254	3.785	291	3.783	288	3.794	272
LiF	4.069	67.2	4.008	70.2	4.035	67.3	4.068	67.3	4.011	72.8	4.018	72.7	3.972	76.3
BN	3.628	374	3.601	407	3.607	401	3.626	370	3.600	402	3.600	402	3.592	410
SiC	4.384	213	4.352	242	4.361	236	4.380	210	4.347	231	4.348	230	4.346	229

[a]Reference 44 (see Erratum for HSE06 results).

ment between the two codes for the bulk modulus. On average, the hybrid functional PBE0 improves over the GGA PBE for the lattice constant and bulk modulus of semiconductors and metals as shown in Ref. 44.

3. YS-PBE0 calculations

As mentioned in Sec. III (see Fig. 2), choosing $\lambda = (3/2)\,\mu$ in Eq. (34) leads to a splitting of the Coulomb operator which is very similar to the one obtained by using the error function with a given μ.[77–79] In the HSE06 functional,[45] μ is fixed to 0.11 bohr^{-1} and in order to see how well the YS-PBE0 functional can reproduce the HSE06 transition energies (see Erratum of Ref. 44), calculations with $\lambda = (3/2)\,0.11 = 0.165$ bohr^{-1} were done. From the results shown in Table II, we can see that the agreement between HSE06 (VASP) and YS-PBE0 is as good as it was for PBE0 with differences smaller than 0.03 eV in most cases. Compared to PBE0, the screened hybrid functionals lead to better (worse) agreement with experiment for small (large)

TABLE IV: Band gap (in eV) and Cu EFG (in 10^{21} V/m^2) of Cu_2O calculated at the experimental lattice constant (4.27 Å).

		EFG		
Method	Band gap	Total	*p-p*	*d-d*
LDA	0.53	−5.3	−16.0	10.5
PBE	0.53	−5.5	−16.4	10.6
B88PW91	0.55	−5.6	−16.4	10.6
EV93PW91	0.57	−6.6	−17.4	10.6
LDA+U (FLL, $U = 4$ eV)	0.65	−6.1	−16.1	9.8
LDA+U (FLL, $U = 8$ eV)	0.80	−6.6	−16.4	9.5
LDA+U (FLL, $U = 12$ eV)	0.91	−7.6	−16.5	8.8
LDA+U (AMF, $U = 4$ eV)	0.63	−4.8	−16.0	11.0
LDA+U (AMF, $U = 8$ eV)	0.79	−2.6	−16.2	13.4
LDA+U (AMF, $U = 12$ eV)	0.94	0.6	−16.6	17.0
PBE0 (onsite)	0.79	−3.4	−16.4	12.8
PBE0	2.77	−8.5	−19.5	10.8
YS-PBE0	1.99	−8.3	−19.3	10.8
pseudo-SIC[a]	1.80			
B3LYP[b]	2.1			
HSE ($\alpha_x = 0.275$)[c]	2.12			
scGW[d]	1.97			
Expt.	2.17[e]	9.8[f]		

[a]Reference 99.
[b]Reference 96.
[c]Reference 101.
[d]References 102.
[e]References 105.
[f]Only the magnitude is known. Calculated using $Q(^{63}\mathrm{Cu}) = 0.22$.[106,107]

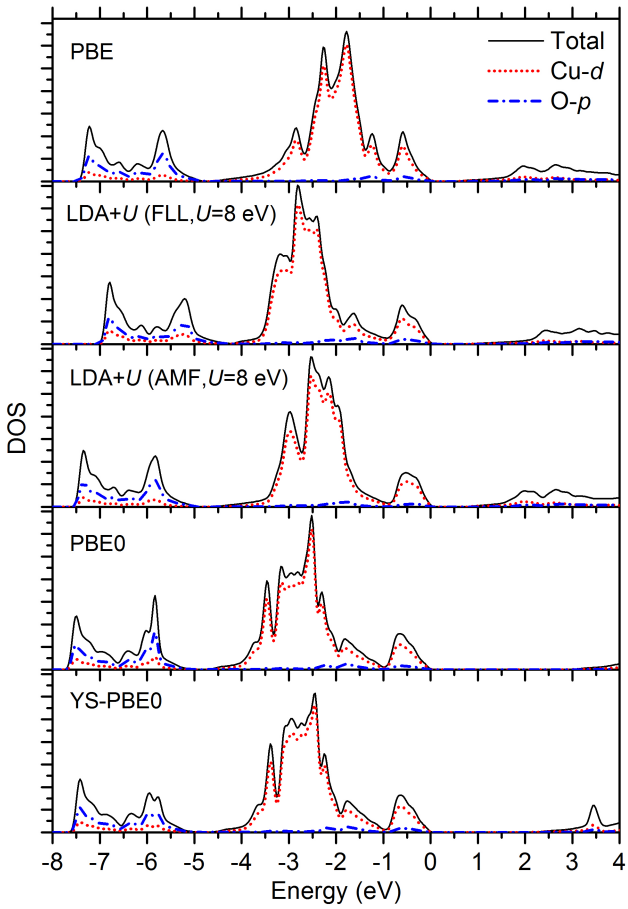

FIG. 4: (Color online) Density of states of Cu_2O calculated with different functionals. The Fermi energy is set at $E = 0$ eV.

band gaps (see also Ref. 47).

The YS-PBE0 results for the lattice constant and bulk modulus are shown in Table III. The agreement between the HSE06 and YS-PBE0 results is fairly good in cases like Li or C, while larger differences can be seen for Si (0.024 Å), LiF (0.017 Å), Cu (0.016 Å), and Rh (0.016 Å). An important contribution to these differences in the lattice constant between the HSE06 and YS-PBE0 values could be attributed to the different schemes used for the screening of the semilocal exchange term [Eq. (35)]. For YS-PBE0, the method of Iikura *et al.*[81] is used, while in HSE06 the screened exchange energy is obtained by integrating a model of the exchange hole.[39,83] However, it seems that using one of the scheme or the other has very little influence on the transition energies as shown above.

B. Cu_2O

Cuprous oxide (Cu_2O) is a semiconductor which has been used in many applications (e.g., catalysis and photovoltaics). Its structure is cubic (space group $Pn\bar{3}m$) and the unit cell, which has a lattice constant of 4.27 Å,[93] contains six atoms. In this structure, shown in Fig. 1 of Ref. 94, the O atoms are fourfold coordinated by Cu atoms, whereas the Cu atoms are linearly coordinated by O atoms. Formally Cu has a valency of +1 and the Cu-3d shell in Cu_2O is full, therefore the correlation effects in the Cu-3d shell should not play an important role as it is the case for CuO.[95]

Many experimental and theoretical studies on Cu_2O have been done. On the theoretical side it has been shown that the semilocal approximations underestimate the band gap as expected (see Refs. 96 and 97 for collections of previously done calculations), but also the Cu electric-field gradient (EFG),[98] which is a ground-state property derived from the electron density. LDA+U (or GGA+U) improves only slightly over the semilocal approximations,[97,98] while the pseudo self-interaction method (pseudo-SIC),[99] the hybrid functionals,[96,100,101] and self-consistent GW (scGW)[102] provide band gaps in much better agreement with experiment. Actually, the results for the EFG show that the semilocal and LDA+U methods do not provide an accurate description of the occupied states.

In Table IV, we show the results for the band gap

and EFG obtained with the hybrid functionals PBE0 and YS-PBE0 ($\lambda = 0.165$ bohr^{-1}), which were obtained with a mesh of $5 \times 5 \times 5$ **k**-points. The calculations with the semilocal (LDA,[92] PBE,[4] B88PW91,[3,88] and EV93PW91[3,103]), LDA+U [fully localized limit (FLL)[104] and around mean-field (AMF)[104] versions], and onsite PBE0[51] methods (results in Table IV) were done with a $12 \times 12 \times 12$ **k**-mesh. The radii of the Cu and O atomic spheres are 1.84 and 1.63 bohr, respectively. LDA, PBE, and B88PW91 give values for the band gap ($\sim$ 0.5 eV) and EFG ($\sim -5.5 \times 10^{21}$ V/m^2) which are much smaller than the experimental values (above 2 eV for the band gap[105] and 9.8×10^{21} V/m^2 for the EFG[106,107]). EV93PW91 improves for the EFG with a value of -6.6×10^{21} V/m^2, but not for the band gap contrary to what was reported for many other solids in Ref. 108. LDA+U slightly improves the results for the band gap and its two versions, FLL and AMF, lead to the same value for a given value of the Coulomb parameter U (the exchange parameter J has been fixed to 0.95 eV). However, this improvement is minor and even with $U = 12$ eV the band gap remains well below the experimental value. For the EFG, FLL and AMF lead to different trends. An increase of U leads to an increase of the magnitude of the EFG with FLL, while the opposite is obtained with AMF, which yields a positive value for $U = 12$ eV. In Table IV, the p-p and d-d components (inside the Cu atomic sphere) of the EFG are also shown. As expected, the change in the EFG due to U comes mainly from the d-d part. The onsite PBE0 method slightly improves the results for the band gap (0.8 eV), but significantly decreases the EFG (-3.4×10^{21} V/m^2). Overall, the FLL version of LDA+U leads to a moderate improvement over the semilocal functionals, while AMF and onsite PBE0 behave similarly by reducing the magnitude of the EFG.

The results obtained with PBE0 and YS-PBE0 are in much better agreement with experiment. In particular, the screened YS-PBE0 functional leads to a band gap of 1.99 eV, which is very close to the experimental value, and an EFG of -8.3×10^{21} V/m^2 which is much closer to experiment compared to the values obtained with other functionals. PBE0 leads to a band gap which seems to be too high and an EFG very similar to YS-PBE0. Focusing now on the PBE and PBE0 results for the EFG, we can see from the decomposition of the EFG (Table IV) that the increase in magnitude of the EFG by going from PBE to PBE0 comes mainly from the p-p component. By decomposing further the p-p component, we could see that the sub-component from the Cu-4p states (which actually originate mainly from a re-expansion of the O-2p tails) is more negative than the total p-p and that the sub-component from the low-lying (~ -5 Ry) semicore Cu-3p states is small and positive. From this we could also determine that the more negative PBE0 p-p component come half and half from the Cu-3p and Cu-4p states.

Figure 4 shows the density of states (DOS) of Cu_2O for a few selected functionals. We can see that in the energy range between -8 and -5 eV below the Fermi energy (set at $E = 0$ eV), most of the DOS comes from O-2p electrons. The DOS between -4 and 0 eV is entirely due to Cu-3d states, while above the band gap, the different partial DOSs actually represent Cu-4s states. By comparing the different functionals, we can observe that the O-2p peaks are higher in energy (closer to the Cu-3d states) for the FLL version of LDA+U. Also, the LDA+U and hybrid methods shift the main Cu-3d peaks down in energy.

Compared to the other hybrid results from the literature (also shown in Table IV), we can see that the HSE (with $\alpha_x = 0.275$) band gap of 2.12 eV[101] is close to the YS-PBE0 value of 1.99 eV, as expected from the results obtained in Sec. IV A 3. The B3LYP band gap of 2.1 eV reported in Ref. 96 is much smaller than our PBE0 value of 2.77 eV. This is mainly due to the smaller amount of HF exchange α_x in B3LYP (0.2 for B3LYP versus 0.25 for PBE0).

V. SUMMARY

The implementation of unscreened and screened hybrid functionals into the WIEN2K code, which is based on the LAPW basis set, has been presented. The screening is based on the Yukawa potential for which the expansion in spherical harmonics has a simple expression. Also, it was possible to calculate analytically all integrals which were necessary for the derivation of the various formulas for the pseudocharge method. In order to check the validity of the implementation, first, test calculations were done on systems which do not contain core electrons, such that the total Hartree-Fock energy could be compared with benchmark results from the literature. As a further test of the implementation, the band gap and lattice constant of several solids have been calculated with the hybrid functionals PBE0 and YS-PBE0 which are based on the GGA functional PBE. The results are in very good agreement with the results obtained by other codes. Noticeably, for the screened hybrid functional YS-PBE0, it was possible to find a value of the screening parameter λ such that the results are very close to the results of HSE06, whose screening is based on the error function. Finally, we applied the hybrid functionals to the semiconductor Cu_2O. The results obtained with the unscreened PBE0 and screened YS-PBE0 for the band gap and EFG are much more accurate than the results obtained with semilocal and LDA+U functionals.

Appendix A: Pseudocharge method

In this appendix, the basic formulas of the pseudocharge method are given (Sec. A 1), as well as explicit expressions used for the HF energy (Sec. A 2).

1. Basic formulas

In all-electron calculations, the charge density ρ has large oscillations near the nuclei, therefore its Fourier expansion will converge slowly, making the calculation of the potential v generated by ρ with Fourier transforms inefficient. The idea of the pseudocharge method[58] is to replace the charge density ρ inside the atomic spheres S_α by a smoother one ($\tilde{\rho}$) such that the Fourier expansion of $\tilde{\rho} = \rho_{\mathrm{PW}} + \overline{\rho}$ converges faster. ρ_{PW} is the continuation inside the spheres of the plane waves (PW) representation of the charge density and $\overline{\rho} = \sum_\alpha \overline{\rho}_\alpha$ is zero in the interstitial region. Such a scheme is possible since the potential in the interstitial region created by the charge inside the spheres depends only on the multipole moments $q_{\ell m}^\alpha$ which are defined as follows for the unscreened [Eq. (8)] and screened [Eq. (9)] potentials:

$$q_{\ell m}^\alpha = \int\limits_{\mathrm{S}_\alpha} Y_{\ell m}^* \left(\hat{\mathbf{r}}\right) r^\ell \rho\left(\mathbf{r}\right) d^3 r, \tag{A1}$$

$$q_{\ell m}^\alpha = \frac{(2\ell+1)!!}{\lambda^\ell} \int\limits_{\mathrm{S}_\alpha} Y_{\ell m}^* \left(\hat{\mathbf{r}}\right) i_\ell\left(\lambda r\right) \rho\left(\mathbf{r}\right) d^3 r. \tag{A2}$$

Therefore, $\overline{\rho}_\alpha$ should be chosen such that inside the spheres, the multipole moments of $\tilde{\rho}$ are equal to the multipole moments of the true charge density ρ. After having determined $\tilde{\rho}$, the potential in the interstital region is calculated with

$$v_{\mathrm{I}}(\mathbf{r}) = 4\pi \sum_{\mathbf{G}} \frac{\tilde{\rho}_{\mathbf{G}}}{|\mathbf{G}|^2} e^{\mathrm{i}\mathbf{G}\cdot\mathbf{r}} \tag{A3}$$

and

$$v_{\mathrm{I}}(\mathbf{r}) = 4\pi \sum_{\mathbf{G}} \frac{\tilde{\rho}_{\mathbf{G}}}{|\mathbf{G}|^2 + \lambda^2} e^{\mathrm{i}\mathbf{G}\cdot\mathbf{r}} \tag{A4}$$

for the unscreened and screened potentials, respectively. Then, inside the atomic sphere S_α, the potential is the solution of a Green function problem:

$$\begin{aligned} v_\alpha(\mathbf{r}) &= \int\limits_{\mathrm{S}_\alpha} \rho(\mathbf{r}') G^\alpha\left(\mathbf{r}, \mathbf{r}'\right) d^3 r' \\ &\quad - \frac{R_\alpha^2}{4\pi} \oint\limits_{\mathrm{S}_\alpha} v_{\mathrm{I}}\left(\mathbf{r}'\right) \frac{\partial G^\alpha}{\partial n'}\left(\mathbf{r}, \mathbf{r}'\right) \sin\theta' d\theta' d\phi', \end{aligned} \tag{A5}$$

where the Green function is given by[58,109]

$$G^\alpha\left(\mathbf{r}, \mathbf{r}'\right) = \sum_{\ell=0}^{\infty} \sum_{m=-\ell}^{\ell} G_\ell^\alpha\left(r, r'\right) Y_{\ell m}^*(\hat{\mathbf{r}}') Y_{\ell m}(\hat{\mathbf{r}}), \tag{A6}$$

where

$$G_\ell^\alpha(r, r') = \frac{4\pi}{2\ell+1} \frac{r_<^\ell}{r_>^{\ell+1}} \left(1 - \frac{r_>^{2\ell+1}}{R_\alpha^{2\ell+1}}\right) \tag{A7}$$

or

$$\begin{aligned} G_\ell^\alpha(r, r') &= 4\pi\lambda i_\ell\left(\lambda r_<\right) k_\ell\left(\lambda r_>\right) \\ &\quad \times \left(1 - \frac{k_\ell\left(\lambda R_\alpha\right) i_\ell\left(\lambda r_>\right)}{i_\ell\left(\lambda R_\alpha\right) k_\ell\left(\lambda r_>\right)}\right) \end{aligned} \tag{A8}$$

for the unscreened and screened potentials, respectively. $\partial G^\alpha / \partial n'$ is the normal derivative of G^α at the sphere boundary.

2. Explicit expressions for the Hartree-Fock energy

In Eqs. (18) and (19), the Fourier coefficients of the pseudocharge density are given by

$$\tilde{\rho}_{n\mathbf{k}n'\mathbf{k}'}^{\sigma\mathbf{q}} = \rho_{n\mathbf{k}n'\mathbf{k}'}^{\sigma\mathbf{G}} + \overline{\rho}_{n\mathbf{k}n'\mathbf{k}'}^{\sigma\mathbf{q}}, \tag{A9}$$

where (unscreened case)

$$\begin{aligned} \overline{\rho}_{n\mathbf{k}n'\mathbf{k}'}^{\sigma\mathbf{q}} &= \frac{4\pi}{\Omega} \sum_\alpha^{\mathrm{cell}} \sum_{\ell,m} \frac{(2\ell+2p+3)!!}{R_\alpha^{\ell+p+1}} \frac{(-\mathrm{i})^\ell}{(2\ell+1)!!} \\ &\quad \times \frac{j_{\ell+p+1}\left(|\mathbf{q}| R_\alpha\right)}{|\mathbf{q}|^{p+1}} e^{-\mathrm{i}\mathbf{q}\cdot\tau_\alpha} Y_{\ell m}\left(\widehat{\mathbf{q}}\right) \overline{q}_{\ell m}^{\alpha\sigma n\mathbf{k}n'\mathbf{k}'} \end{aligned} \tag{A10}$$

or (screened case)

$$\begin{aligned} \overline{\rho}_{n\mathbf{k}n'\mathbf{k}'}^{\sigma\mathbf{q}} &= \frac{4\pi}{\Omega} \sum_\alpha^{\mathrm{cell}} \sum_{\ell,m} \frac{\lambda^{\ell+p+1}}{i_{\ell+p+1}\left(\lambda R_\alpha\right)} \frac{(-\mathrm{i})^\ell}{(2\ell+1)!!} \\ &\quad \times \frac{j_{\ell+p+1}\left(|\mathbf{q}| R_\alpha\right)}{|\mathbf{q}|^{p+1}} e^{-\mathrm{i}\mathbf{q}\cdot\tau_\alpha} Y_{\ell m}\left(\widehat{\mathbf{q}}\right) \overline{q}_{\ell m}^{\alpha\sigma n\mathbf{k}n'\mathbf{k}'}. \end{aligned} \tag{A11}$$

In Eqs. (A10) and (A11), p is an integer which is chosen such that $\ell + p$ is fixed.[58] For $\mathbf{q} = \mathbf{0}$, Eqs. (A10) and (A11) reduce to

$$\overline{\rho}_{n\mathbf{k}n'\mathbf{k}}^{\sigma\mathbf{0}} = \frac{\sqrt{4\pi}}{\Omega} \sum_\alpha^{\mathrm{cell}} \overline{q}_{00}^{\alpha\sigma n\mathbf{k}n'\mathbf{k}} \tag{A12}$$

and

$$\overline{\rho}_{n\mathbf{k}n'\mathbf{k}}^{\sigma\mathbf{0}} = \frac{\sqrt{4\pi}}{\Omega} \sum_\alpha^{\mathrm{cell}} \frac{(\lambda R_\alpha)^{p+1}}{(2p+3)!! i_{p+1}\left(\lambda R_\alpha\right)} \overline{q}_{00}^{\alpha\sigma n\mathbf{k}n'\mathbf{k}}, \tag{A13}$$

respectively. In Eqs. (A10)-(A13),

$$\overline{q}_{\ell m}^{\alpha\sigma n\mathbf{k}n'\mathbf{k}'} = q_{\ell m}^{\alpha\sigma n\mathbf{k}n'\mathbf{k}'} - q_{\ell m}^{\mathrm{PW},\alpha\sigma n\mathbf{k}n'\mathbf{k}'}, \tag{A14}$$

where $q_{\ell m}^{\alpha\sigma n\mathbf{k}n'\mathbf{k}'}$ and $q_{\ell m}^{\mathrm{PW},\alpha\sigma n\mathbf{k}n'\mathbf{k}'}$ are the multipole moments of $\rho_{n\mathbf{k}n'\mathbf{k}'}^\sigma$ inside the spheres and of the continuation of the PW representation of $\rho_{n\mathbf{k}n'\mathbf{k}'}^\sigma$ inside the

spheres, respectively, whose expressions are given by

$$q_{\ell m}^{\alpha\sigma n\mathbf{k}n'\mathbf{k}'} = \sum_{\ell_1,\ell_2}\sum_{f_1,f_2} T_{\alpha\sigma n\mathbf{k}n'\mathbf{k}'}^{f_1 f_2 \ell_1 \ell_2 \ell m} \times \int_0^{R_\alpha} u_{f_1\ell_1}^{\alpha\sigma}(r) u_{f_2\ell_2}^{\alpha\sigma}(r) r^{\ell+2} dr \quad \text{(A15)}$$

$$q_{\ell m}^{\mathrm{PW},\alpha\sigma n\mathbf{k}n'\mathbf{k}'} = \sum_{\mathbf{G}} \frac{4\pi \mathrm{i}^\ell R_\alpha^{\ell+2} j_{\ell+1}\left(|\mathbf{q}|\, R_\alpha\right)}{|\mathbf{q}|} \times e^{\mathrm{i}\mathbf{q}\cdot\tau_\alpha} Y_{\ell m}^*\left(\widehat{\mathbf{q}}\right) \rho_{n\mathbf{k}n'\mathbf{k}'}^{\sigma\mathbf{G}} \quad \text{(A16)}$$

for the unscreened potential and

$$q_{\ell m}^{\alpha\sigma n\mathbf{k}n'\mathbf{k}'} = \frac{(2\ell+1)!!}{\lambda^\ell} \sum_{\ell_1,\ell_2}\sum_{f_1,f_2} T_{\alpha\sigma n\mathbf{k}n'\mathbf{k}'}^{f_1 f_2 \ell_1 \ell_2 \ell m} \times \int_0^{R_\alpha} u_{f_1\ell_1}^{\alpha\sigma}(r) u_{f_2\ell_2}^{\alpha\sigma}(r) i_\ell\left(\lambda r\right) r^2 dr \quad \text{(A17)}$$

$$q_{\ell m}^{\mathrm{PW},\alpha\sigma n\mathbf{k}n'\mathbf{k}'} = \sum_{\mathbf{G}} \left[\lambda j_\ell\left(|\mathbf{q}|\, R_\alpha\right) i_{\ell-1}\left(\lambda R_\alpha\right) - |\mathbf{q}|\, j_{\ell-1}\left(|\mathbf{q}|\, R_\alpha\right) i_\ell\left(\lambda R_\alpha\right)\right] \frac{4\pi \mathrm{i}^\ell R_\alpha^2 (2\ell+1)!!}{\lambda^\ell\left(|\mathbf{q}|^2+\lambda^2\right)} e^{\mathrm{i}\mathbf{q}\cdot\tau_\alpha} Y_{\ell m}^*\left(\widehat{\mathbf{q}}\right) \rho_{n\mathbf{k}n'\mathbf{k}'}^{\sigma\mathbf{G}} \quad \text{(A18)}$$

for the screened potential. When $\mathbf{k}=\mathbf{k}'$, the term $\mathbf{G}=\mathbf{0}$ in Eqs. (A16) and (A18) reduces to

$$\delta_{\ell 0}\sqrt{4\pi}\frac{R_\alpha^3}{3}\rho_{n\mathbf{k}n'\mathbf{k}}^{\sigma\mathbf{0}} \quad \text{(A19)}$$

and

$$\delta_{\ell 0}\sqrt{4\pi}\frac{R_\alpha^2 i_1\left(\lambda R_\alpha\right)}{\lambda}\rho_{n\mathbf{k}n'\mathbf{k}}^{\sigma\mathbf{0}}, \quad \text{(A20)}$$

respectively.

Appendix B: Total energy

For the case of a hybrid exchange-correlation functional, the total energy is given by (spin-unpolarized form)

$$E_{\mathrm{tot}} = T_{\mathrm{s}} + \frac{1}{2}\int_{\mathrm{cell}} v_{\mathrm{Coul}}(\mathbf{r})\rho(\mathbf{r}) d^3r - \frac{1}{2}\sum_\alpha^{\mathrm{cell}} Z_\alpha v_{\mathrm{M}}^\alpha(\tau_\alpha) + E_{\mathrm{xc}}^{\mathrm{SL}} + \alpha_{\mathrm{x}}\left(E_{\mathrm{x}}^{\mathrm{HF}} - E_{\mathrm{x}}^{\mathrm{SL}}\right), \quad \text{(B1)}$$

where T_{s} is the kinetic energy of the electrons and

$$v_{\mathrm{Coul}}(\mathbf{r}) = \int_{\mathrm{crystal}} \frac{\rho(\mathbf{r}')}{|\mathbf{r}-\mathbf{r}'|} d^3r' - \sum_\beta^{\mathrm{crystal}} \frac{Z_\beta}{|\mathbf{r}-\tau_\beta|}, \quad \text{(B2)}$$

$$v_{\mathrm{M}}^\alpha(\tau_\alpha) = \int_{\mathrm{crystal}} \frac{\rho(\mathbf{r}')}{|\tau_\alpha-\mathbf{r}'|} d^3r' - \sum_{\substack{\beta \\ \beta\neq\alpha}}^{\mathrm{crystal}} \frac{Z_\beta}{|\tau_\alpha-\tau_\beta|}, \quad \text{(B3)}$$

are the Coulomb and Madelung potentials, respectively. By using the sum of the eigenvalues

$$\sum_{n_{\mathrm{c}},\ell_{\mathrm{c}},m_{\mathrm{c}}} \epsilon_{n_{\mathrm{c}}\ell_{\mathrm{c}}m_{\mathrm{c}}} + \sum_{n,\mathbf{k}} w_{n\mathbf{k}}\epsilon_{n\mathbf{k}} = T_{\mathrm{s}} + \int_{\mathrm{cell}} v_{\mathrm{Coul}}(\mathbf{r})\rho(\mathbf{r}) d^3r + \int_{\mathrm{cell}} v_{\mathrm{xc}}^{\mathrm{SL}}(\mathbf{r})\rho(\mathbf{r}) d^3r + \alpha_{\mathrm{x}}\left(2E_{\mathrm{x,vv}}^{\mathrm{HF}} + E_{\mathrm{x,vc}}^{\mathrm{HF}} - \int_{\mathrm{cell}} v_{\mathrm{x}}^{\mathrm{SL}}(\mathbf{r})\rho_{\mathrm{val}}(\mathbf{r}) d^3r\right), \quad \text{(B4)}$$

where ρ_{val} is the valence electron density (the core electrons experience the semilocal potential), the total energy can be rewritten as

$$E_{\mathrm{tot}} = \sum_{n_{\mathrm{c}},\ell_{\mathrm{c}},m_{\mathrm{c}}} \epsilon_{n_{\mathrm{c}}\ell_{\mathrm{c}}m_{\mathrm{c}}} + \sum_{n,\mathbf{k}} w_{n\mathbf{k}}\epsilon_{n\mathbf{k}} - \frac{1}{2}\int_{\mathrm{cell}} v_{\mathrm{Coul}}(\mathbf{r})\rho(\mathbf{r}) d^3r - \frac{1}{2}\sum_\alpha^{\mathrm{cell}} Z_\alpha v_{\mathrm{M}}^\alpha(\tau_\alpha) - \int_{\mathrm{cell}} v_{\mathrm{xc}}^{\mathrm{SL}}(\mathbf{r})\rho(\mathbf{r}) d^3r$$

$$+E_{\rm xc}^{\rm SL}+\alpha_{\rm x}\left(E_{\rm x,cc}^{\rm HF}-E_{\rm x,vv}^{\rm HF}+\int\limits_{\rm cell} v_{\rm x}^{\rm SL}(\mathbf{r})\rho_{\rm val}(\mathbf{r})d^3r-E_{\rm x}^{\rm SL}\right). \quad \text{(B5)}$$

For a screened hybrid functional, the exchange-only terms are simply replaced by their SR counterparts. The use of the second variational procedure allows us to write the sum of the valence eigenvalues in the following way:

$$\sum_{n,\mathbf{k}} w_{n\mathbf{k}}\epsilon_{n\mathbf{k}} = \sum_{n,\mathbf{k}} w_{n\mathbf{k}} \sum_m |c_{n\mathbf{k}}^m|^2 \epsilon_{m\mathbf{k}}^{\rm SL} + \alpha_{\rm x}\left(2E_{\rm x,vv}^{\rm HF} + E_{\rm x,vc}^{\rm HF} - \int\limits_{\rm cell} v_{\rm x}^{\rm SL}(\mathbf{r})\rho_{\rm val}(\mathbf{r})d^3r\right), \quad \text{(B6)}$$

where $c_{n\mathbf{k}}^m$ are the coefficients of the expansion of $\psi_{n\mathbf{k}}$ ($\psi_{n\mathbf{k}} = \sum_m c_{n\mathbf{k}}^m \psi_{m\mathbf{k}}^{\rm SL}$). From Eq. (B6), the valence-valence HF exchange energy $E_{\rm x,vv}^{\rm HF}$ can be calculated, thus avoiding the use of Eq. (2), which is the most expensive component of the total energy to calculate.

Appendix C: Functional derivative of $E_{\rm x}^{\rm SR\text{-}SL}$

The functional derivative of $E_{\rm x}^{\rm SR\text{-}SL}$ [Eq. (35)] for the spin-unpolarized case is given by

$$v_{\rm x}^{\rm SR\text{-}SL} = -\frac{3}{4}\left(\frac{3}{\pi}\right)^{1/3}\left(v_1 J + v_2\frac{dJ}{da} + v_3\frac{d^2J}{da^2}\right), \quad \text{(C1)}$$

where

$$v_1 = \frac{4}{3}\rho^{1/3}F_{\rm x} - \frac{1}{b^2}\frac{\nabla^2\rho}{\rho^{4/3}}H_{\rm x} + \left(\frac{4}{3}\rho^{1/3}s^3 - \frac{1}{b^3}\frac{t}{\rho^{8/3}}\right)\frac{dH_{\rm x}}{ds}, \quad \text{(C2)}$$

$$v_2 = -\frac{1}{3}\frac{\lambda}{b}F_{\rm x}^{3/2} + \left(\frac{1}{2}\frac{\lambda}{b}s^2 - \frac{1}{2}\frac{\lambda}{b^3}\frac{\nabla^2\rho}{\rho^{5/3}}\right)F_{\rm x}^{1/2}H_{\rm x} + \left(\frac{2}{3}\frac{\lambda}{b}s^3 - \frac{1}{2}\frac{\lambda}{b^4}\frac{t}{\rho^3}\right)F_{\rm x}^{1/2}\frac{dH_{\rm x}}{ds} + \left(\frac{\lambda}{b}s^4 - \frac{3}{4}\frac{\lambda}{b^4}\frac{st}{\rho^3}\right)\frac{H_{\rm x}^2}{F_{\rm x}^{1/2}}, \quad \text{(C3)}$$

$$v_3 = \frac{1}{6}\frac{\lambda^2}{b^2}\frac{s^2}{\rho^{1/3}}F_{\rm x}H_{\rm x} + \left(\frac{1}{3}\frac{\lambda^2}{b^2}\frac{s^4}{\rho^{1/3}} - \frac{1}{4}\frac{\lambda^2}{b^5}\frac{st}{\rho^{10/3}}\right)H_{\rm x}^2, \quad \text{(C4)}$$

where $b = 2\left(3\pi^2\right)^{1/3}$, $s = |\nabla\rho| / \left(2\left(3\pi^2\right)^{1/3}\rho^{4/3}\right)$, $t = \nabla\rho\cdot\nabla|\nabla\rho|$, and $H_{\rm x} = (1/s)\,dF_{\rm x}/ds$.

Acknowledgments

We are grateful to Robert Laskowski, Sandro Massidda, and Michael Weinert for very useful discussions. This work was supported by the projects P20271-N17 and SFB-F41 (ViCoM) of the Austrian Science Fund.

[1] P. Hohenberg and W. Kohn, Phys. Rev. **136**, B864 (1964).
[2] W. Kohn and L. J. Sham, Phys. Rev. **140**, A1133 (1965).
[3] J. P. Perdew, J. A. Chevary, S. H. Vosko, K. A. Jackson, M. R. Pederson, D. J. Singh, and C. Fiolhais, Phys. Rev. B **46**, 6671 (1992); **48**, 4978 (1993).
[4] J. P. Perdew, K. Burke, and M. Ernzerhof, Phys. Rev. Lett. **77**, 3865 (1996); **78**, 1396 (1997).
[5] F. Tran, R. Laskowski, P. Blaha, and K. Schwarz, Phys. Rev. B **75**, 115131 (2007).
[6] P. Haas, F. Tran, and P. Blaha, Phys. Rev. B **79**, 085104 (2009); **79**, 209902(E) (2009).
[7] S. Kümmel and L. Kronik, Rev. Mod. Phys. **80**, 3 (2008).
[8] M. Städele, M. Moukara, J. A. Majewski, P. Vogl, and A. Görling, Phys. Rev. B **59**, 10031 (1999).
[9] E. Engel and R. N. Schmid, Phys. Rev. Lett. **103**, 036404 (2009).
[10] F. Tran and P. Blaha, Phys. Rev. Lett. **102**, 226401 (2009).
[11] A. Seidl, A. Görling, P. Vogl, J. A. Majewski, and M. Levy, Phys. Rev. B **53**, 3764 (1996).
[12] V. I. Anisimov, J. Zaanen, and O. K. Andersen, Phys. Rev. B **44**, 943 (1991).
[13] D. M. Bylander and L. Kleinman, Phys. Rev. B **41**, 7868 (1990).
[14] A. D. Becke, J. Chem. Phys. **98**, 1372 (1993).
[15] A. D. Becke, J. Chem. Phys. **98**, 5648 (1993).
[16] F. Bechstedt, F. Fuchs, and G. Kresse, Phys. Status Solidi B **246**, 1877 (2009).
[17] E. R. Ylvisaker, W. E. Pickett, and K. Koepernik, Phys. Rev. B **79**, 035103 (2009).
[18] H. Yukawa, Proc. Phys. Math. Soc. Jpn. **17**, 48 (1935).
[19] S. J. Clark and J. Robertson, Phys. Rev. B **82**, 085208 (2010).
[20] B. Lee, L.-W. Wang, C. D. Spataru, and S. G. Louie, Phys. Rev. B **76**, 245114 (2007).
[21] R. Asahi, W. Mannstadt, and A. J. Freeman, Phys. Rev. B **59**, 7486 (1999).
[22] R. Asahi, W. Mannstadt, and A. J. Freeman, Phys. Rev.

B **62**, 2552 (2000).
[23] C. B. Geller, W. Wolf, S. Picozzi, A. Continenza, R. Asahi, W. Mannstadt, A. J. Freeman, and E. Wimmer, Appl. Phys. Lett. **79**, 368 (2001).
[24] L. Dagens and F. Perrot, Phys. Rev. B **5**, 641 (1972).
[25] A. Svane, Phys. Rev. B **35**, 5496 (1987).
[26] C. Pisani, R. Dovesi, and C. Roetti, *Hartree-Fock ab initio Treatment of Crystalline Systems,* Vol. 48 of *Lecture Notes in Chemistry,* edited by G. Berthier, M. J. S. Dewar, H. Fischer, K. Fukui, G. G. Hall, J. Hinze, H. H. Jaffé, J. Jortner, W. Kutzelnigg, K. Ruedenberg, and J. Tomasi (Springer-Verlag, Heidelberg, 1988).
[27] S. Massidda, M. Posternak, and A. Baldereschi, Phys. Rev. B **48**, 5058 (1993).
[28] T. Bredow and A. R. Gerson, Phys. Rev. B **61**, 5194 (2000).
[29] J. Muscat, A. Wander, and N. M. Harrison, Chem. Phys. Lett. **342**, 397 (2001).
[30] J. K. Perry, J. Tahir-Kheli, and W. A. Goddard III, Phys. Rev. B **63**, 144510 (2001).
[31] F. Corà, M. Alfredsson, G. Mallia, D. S. Middlemiss, W. C. Mackrodt, R. Dovesi, and R. Orlando, Struct. Bonding (Berlin) **113**, 171 (2004).
[32] I. de P. R. Moreira, F. Illas, and R. L. Martin, Phys. Rev. B **65**, 155102 (2002).
[33] K. N. Kudin, G. E. Scuseria, and R. L. Martin, Phys. Rev. Lett. **89**, 266402 (2002).
[34] C. Franchini, V. Bayer, R. Podloucky, J. Paier, and G. Kresse, Phys. Rev. B **72**, 045132 (2005).
[35] P. J. Stephens, F. J. Devlin, C. F. Chabalowski, and M. J. Frisch, J. Phys. Chem. **98**, 11623 (1994).
[36] M. Ernzerhof and G. E. Scuseria, J. Chem. Phys. **110**, 5029 (1999).
[37] C. Adamo and V. Barone, J. Chem. Phys. **110**, 6158 (1999).
[38] J. Heyd, G. E. Scuseria, and M. Ernzerhof, J. Chem. Phys. **118**, 8207 (2003); **124**, 219906 (2006).
[39] J. Heyd and G. E. Scuseria, J. Chem. Phys. **120**, 7274 (2004).
[40] J. Heyd and G. E. Scuseria, J. Chem. Phys. **121**, 1187 (2004).
[41] R. D. Adamson, J. P. Dombroski, and P. M. W. Gill, Chem. Phys. Lett. **254**, 329 (1996).
[42] A. Savin, in *Recent Developments and Applications of Modern Density Functional Theory*, edited by J. M. Seminario (Elsevier, Amsterdam, 1996), p. 327.
[43] J. Heyd, J. E. Peralta, G. E. Scuseria, and R. L. Martin, J. Chem. Phys. **123**, 174101 (2005).
[44] J. Paier, M. Marsman, K. Hummer, G. Kresse, I. C. Gerber, and J. G. Ángyán, J. Chem. Phys. **124**, 154709 (2006); **125**, 249901 (2006).
[45] A. V. Krukau, O. A. Vydrov, A. F. Izmaylov, and G. E. Scuseria, J. Chem. Phys. **125**, 224106 (2006).
[46] X. Wu, E. J. Walter, A. M. Rappe, R. Car, and A. Selloni, Phys. Rev. B **80**, 115201 (2009).
[47] M. A. L. Marques, J. Vidal, M. J. T. Oliveira, L. Reining, and S. Botti, Phys. Rev. B **83**, 035119 (2011).
[48] M. Marsman, J. Paier, A. Stroppa, and G. Kresse, J. Phys.: Condens. Matter **20**, 064201 (2008).
[49] M. Guidon, F. Schiffmann, J. Hutter, and J. VandeVondele, J. Chem. Phys. **128**, 214104 (2008).
[50] P. Novák, J. Kuneš, L. Chaput, and W. E. Pickett, Phys. Status Solidi B **243**, 563 (2006).
[51] F. Tran, P. Blaha, K. Schwarz, and P. Novák, Phys. Rev. B **74**, 155108 (2006).
[52] F. Jollet, G. Jomard, B. Amadon, J. P. Crocombette, and D. Torumba, Phys. Rev. B **80**, 235109 (2009).
[53] P. Blaha, K. Schwarz, G. K. H. Madsen, D. Kvasnicka, and J. Luitz, WIEN2K: *An Augmented Plane Wave plus Local Orbitals Program for Calculating Crystal Properties*, edited by K. Schwarz (Vienna University of Technology, Austria, 2001).
[54] O. K. Andersen, Phys. Rev. B **12**, 3060 (1975).
[55] D. J. Singh and L. Nordström, *Planewaves, Pseudopotentials and the LAPW Method*, 2nd ed. (Springer, Berlin, 2006).
[56] E. Sjöstedt, L. Nordström, and D. J. Singh, Solid State Commun. **114**, 15 (2000).
[57] G. K. H. Madsen, P. Blaha, K. Schwarz, E. Sjöstedt, and L. Nordström, Phys. Rev. B **64**, 195134 (2001).
[58] M. Weinert, J. Math. Phys. **22**, 2433 (1981).
[59] A. V. Nikolaev and P. N. Dyachkov, Int. J. Quantum Chem. **89**, 57 (2002); **93**, 375 (2003).
[60] C. Friedrich, A. Schindlmayr, and S. Blügel, Comput. Phys. Commun. **180**, 347 (2009).
[61] M. Betzinger, C. Friedrich, and S. Blügel, Phys. Rev. B **81**, 195117 (2010).
[62] M. Betzinger, C. Friedrich, S. Blügel, and A. Görling, Phys. Rev. B **83**, 045105 (2011).
[63] G. B. Arfken and H. J. Weber, *Mathematical Methods for Physicists*, 6th ed. (Elsevier Academic Press, San Diego, CA, 2005).
[64] J. G. Ángyán, I. Gerber, and M. Marsman, J. Phys. A **39**, 8613 (2006).
[65] F. Gygi and A. Baldereschi, Phys. Rev. B **34**, 4405 (1986).
[66] B. Wenzien, G. Cappellini, and F. Bechstedt, Phys. Rev. B **51**, 14701 (1995).
[67] J. Paier, R. Hirschl, M. Marsman, and G. Kresse, J. Chem. Phys. **122**, 234102 (2005).
[68] P. Carrier, S. Rohra, and A. Görling, Phys. Rev. B **75**, 205126 (2007).
[69] J. Spencer and A. Alavi, Phys. Rev. B **77**, 193110 (2008).
[70] A. Sorouri, W. M. C. Foulkes, and N. D. M. Hine, J. Chem. Phys. **124**, 064105 (2006).
[71] I. Duchemin and F. Gygi, Comput. Phys. Commun. **181**, 855 (2010).
[72] H.-V. Nguyen and S. de Gironcoli, Phys. Rev. B **79**, 205114 (2009).
[73] P. Broqvist, A. Alkauskas, and A. Pasquarello, Phys. Rev. B **80**, 085114 (2009).
[74] J. Paier, C. V. Diaconu, G. E. Scuseria, M. Guidon, J. VandeVondele, and J. Hutter, Phys. Rev. B **80**, 174114 (2009); B. Civalleri, R. Orlando, C. M. Zicovich-Wilson, C. Roetti, V. R. Saunders, C. Pisani, and R. Dovesi, *ibid.* **81**, 106101 (2010).
[75] J. Harl, L. Schimka, and G. Kresse, Phys. Rev. B **81**, 115126 (2010).
[76] J. Toulouse, F. Colonna, and A. Savin, Phys. Rev. A **70**, 062505 (2004).
[77] T. Shimazaki and Y. Asai, Chem. Phys. Lett. **466**, 91 (2008).
[78] T. Shimazaki and Y. Asai, J. Chem. Phys. **130**, 164702 (2009).
[79] T. Shimazaki and Y. Asai, J. Chem. Phys. **132**, 224105 (2010).
[80] J. E. Robinson, F. Bassani, R. S. Knox, and J. R. Schrieffer, Phys. Rev. Lett. **9**, 215 (1962).

[81] H. Iikura, T. Tsuneda, T. Yanai, and K. Hirao, J. Chem. Phys. **115**, 3540 (2001).
[82] Y. Akinaga and S. Ten-no, Chem. Phys. Lett. **462**, 348 (2008).
[83] M. Ernzerhof and J. P. Perdew, J. Chem. Phys. **109**, 3313 (1998).
[84] T. M. Henderson, B. G. Janesko, and G. E. Scuseria, J. Chem. Phys. **128**, 194105 (2008).
[85] L. Schimka, J. Harl, and G. Kresse, J. Chem. Phys. **134**, 024116 (2011).
[86] J. P. Perdew, A. Ruzsinszky, G. I. Csonka, O. A. Vydrov, G. E. Scuseria, L. A. Constantin, X. Zhou, and K. Burke, Phys. Rev. Lett. **100**, 136406 (2008); **102** 039902(E) (2009); A. E. Mattsson, R. Armiento, and T. R. Mattsson, *ibid.* **101**, 239701 (2008); J. P. Perdew, A. Ruzsinszky, G. I. Csonka, O. A. Vydrov, G. E. Scuseria, L. A. Constantin, X. Zhou, and K. Burke, *ibid.* **101**, 239702 (2008).
[87] J. P. Perdew, M. Ernzerhof, and K. Burke, J. Chem. Phys. **105**, 9982 (1996).
[88] A. D. Becke, Phys. Rev. A **38**, 3098 (1988).
[89] T. Zhu, C. Lee, and W. Yang, J. Chem. Phys. **98**, 4814 (1993).
[90] A. D. Becke and E. R. Johnson, J. Chem. Phys. **127**, 124108 (2007).
[91] C. Froese Fischer, *The Hartree-Fock Method for Atoms: A Numerical Approach* (Wiley, New York, 1977).
[92] J. P. Perdew and Y. Wang, Phys. Rev. B **45**, 13244 (1992).
[93] A. Werner and H. D. Hochheimer, Phys. Rev. B **25**, 5929 (1982).
[94] P. Marksteiner, P. Blaha, and K. Schwarz, Z. Phys. B: Condens. Matter **64**, 119 (1986).
[95] J. Ghijsen, L. H. Tjeng, J. van Elp, H. Eskes, J. Westerink, G. A. Sawatzky, and M. T. Czyzyk Phys. Rev. B **38**, 11322 (1988).
[96] J. P. Hu, D. J. Payne, R. G. Egdell, P.-A. Glans, T. Learmonth, K. E. Smith, J. Guo, and N. M. Harrison, Phys. Rev. B **77**, 155115 (2008).
[97] D. O. Scanlon, B. J. Morgan, and G. W. Watson, J. Chem. Phys. **131**, 124703 (2009).
[98] R. Laskowski, P. Blaha, and K. Schwarz, Phys. Rev. B **67**, 075102 (2003).
[99] A. Filippetti and V. Fiorentini, Phys. Rev. B **72**, 035128 (2005).
[100] D. O. Scanlon, B. J. Morgan, G. W. Watson, and A. Walsh, Phys. Rev. Lett. **103**, 096405 (2009).
[101] D. O. Scanlon and G. W. Watson, J. Phys. Chem. Lett. **1**, 2582 (2010).
[102] F. Bruneval, N. Vast, L. Reining, M. Izquierdo, F. Sirotti, and N. Barrett, Phys. Rev. Lett. **97**, 267601 (2006).
[103] E. Engel and S. H. Vosko, Phys. Rev. B **47**, 13164 (1993).
[104] M. T. Czyżyk and G. A. Sawatzky, Phys. Rev. B **49**, 14211 (1994).
[105] P. W. Baumeister, Phys. Rev. **121**, 359 (1961).
[106] T. Kushida, G. B. Benedek, and N. Bloembergen, Phys. Rev. **104**, 1364 (1956).
[107] P. Pyykkö, Mol. Phys. **99**, 1617 (2001).
[108] F. Tran, P. Blaha, and K. Schwarz, J. Phys.: Condens. Matter **19**, 196208 (2007).
[109] J. D. Jackson, *Classical Electrodynamics*, 3rd ed. (Wiley, New York, 1999).